Design of Ultralight Aircraft

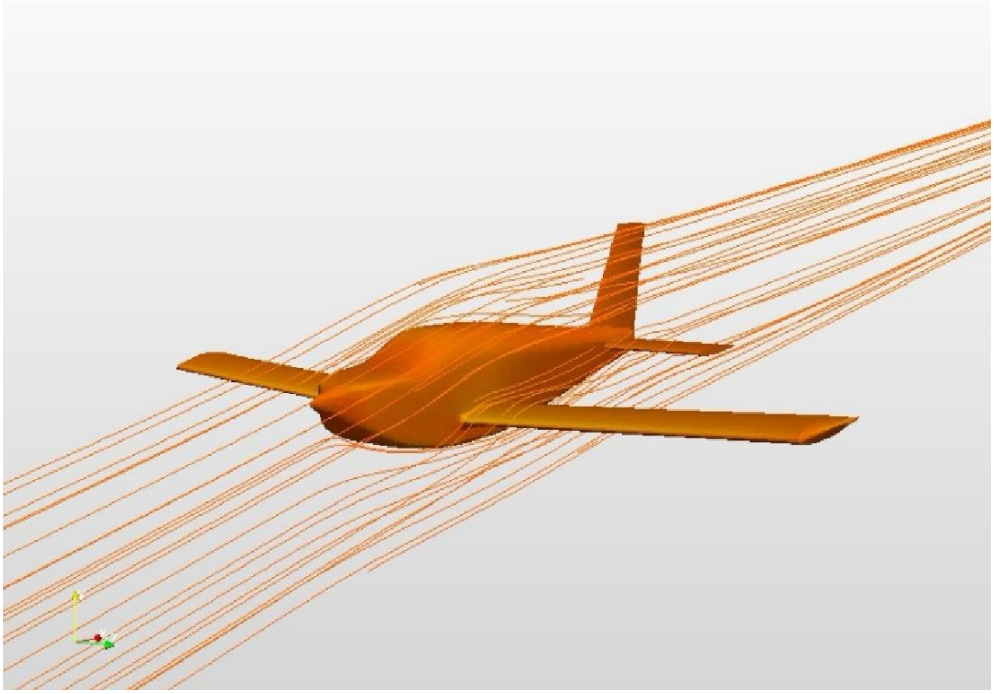

Greece 2018

Main purpose of present study

The purpose of this study is to design and develop a new aircraft that complies with the European ultra-light aircraft regulations and the US Light Sport Aircraft regulation. For the design and development of the aircraft all tools available to the modern engineer have been properly used. The aircraft is a two-seater model, oriented towards fast and economic travelling. For this purpose, the development of the wings, the propeller and fuselage has been done with extra caution, in order for us to achieve the best results possible.

The Design Process

The procedure below is the one that was followed:

1) The airfoil was chosen with the help of xfoil, in order to completely meet the requirements. The results were analyzed by a two-dimensional analysis that was carried out using the openfoam CFD program.
2) Then, the first 3D simulation of the digital model was carried out using the vortex lattice method. At that point, the selection of the design of the aircraft and the aileron wing dimensions for the rudder and the elevator were made, in such a way that economy, maximum performance and safe flight are equally achieved. The results were checked with OpenFoam.
3) With the help of the LISA program, the Finite Element Analysis of the aircraft was performed. The wings and the airframe were designed to be able to carry the design loads resulting from the regulations above.
4) At this stage, the weight distribution of the aircraft finally became known. The Static and Dynamic Stability Analysis was carried out with the help of the VLM program.
5) By using the OpenFoam program the final and precise analysis of the aircraft's aerodynamics was carried out. The aircraft's stall behavior was analyzed - at maximum speed and in all flight combinations- and then the results of the analysis were evaluated. Additionally, the aircraft's propeller was also designed.
6) A modal analysis was performed in order to calculate the wings' natural frequencies. With the wings' aerodynamic data known with the help of LISA, a divergence and control reversal analysis was performed. An unsteady analysis was carried out in OpenFoam in order to calculate the around-the-aircraft unstable load due to turbulence. The results were evaluated in accordance with the natural frequencies that were previously calculated with the help of Lisa, and then a flatter test was performed.
7) With the help of the Code_Aster program, an elasto-plastic analysis of the fuselage was carried out, in the event of a collision.
8) The aircraft's technical characteristics.

1) Airfoil design

As it has already been mentioned, once the aircraft design objective has been established, the primary topic of study for the engineer is the airfoil. For this specific aircraft, whose goal is directed towards fast and economic travels at the flight level of 8000-12000 feet, the ideal for this purpose airfoil was chosen. This airfoil has a particularly low drag when it comes to travel conditions, but if it was to be manufactured in a way that would allow the use of negative flaps, it may maintain both a low drag and an ideal buoyant force, even at high speeds. This is very important, because it is possible for an airfoil to have a low drag, even at a high speed, but to also be able to exert a large buoyant force, which will compel the aircraft to move with a negative pitch in order to maintain its flight level, which will also lead to an increase of the rest of the aircraft's drag coefficient, along with a simultaneous increase in travel costs and decrease in maximum speed.

Below are figures of the analysis made in FORTRAN environment and the resulting graphs.

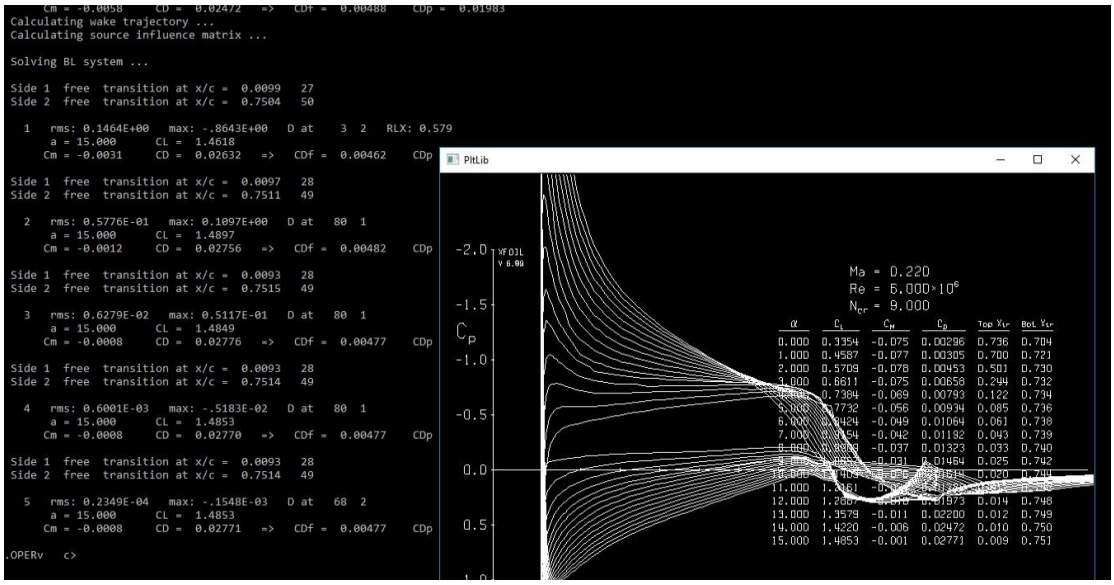

Figure 1.1: The figure above shows the analysis results in xfoil

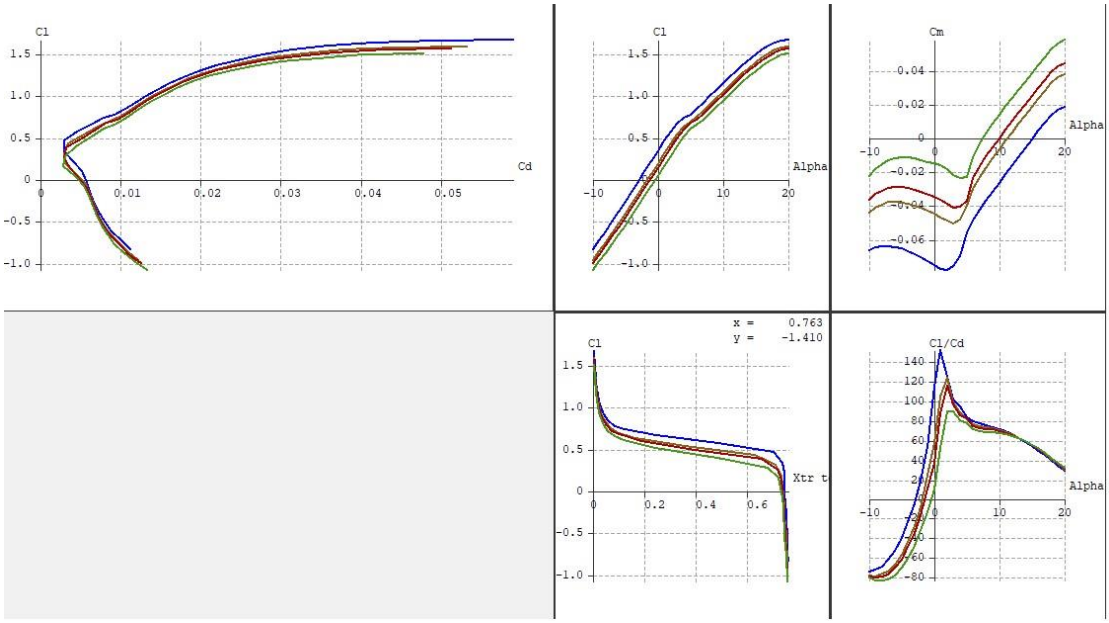

Figure 1.2: The figure above shows the results in a graphics environment. Analyses for negative flap positions were performed, resulting in the creation of an area of constant drag (less than 3 per thousand). At the same time, the value of the buoyancy coefficient varied in order to guarantee the horizontal motion of the aircraft. This airfoil is ideal for this study's aircraft.

2) 3d vlm aircraft analysis

The airfoil selection was made in the previous section, based on the results of a two-dimensional analysis. This happened in order for us to be able to reduce calculation time and to settle on the ideal airfoil, easily and economically.

In this section, an analysis of the aircraft as an entity in space will be carried out for the first time - in other words, a three-dimensional analysis. When this analysis has been completed (at this stage, many configuration tests will take place in order for us to settle on a design that has the optimal characteristics), the not-quite-final design of the aircraft will be selected. It is not quite final yet, because the geometric characteristics may change during the aircraft's stability testing. Weight distribution has not been finalized just yet and that is why a stability testing cannot be done at this stage of the design. It will be finalized, though, after the finite element analysis that follows. The results will also be verified by OpenFoam. It will be checked whether it meets the study's requirements, drag in cruise conditions, of maximum speed and satisfactory buoyance with full-range flaps that will ensure a maximum stall speed in order to meet the criteria of the European Light Aircraft regulation and also to reach high performance while saving fuel.

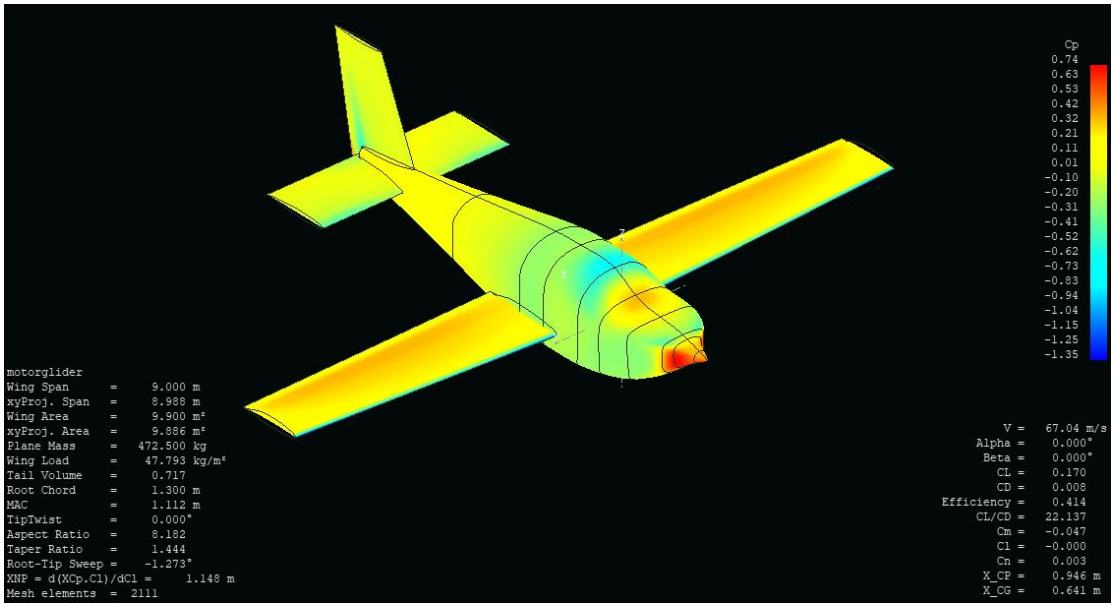

Figure 2.1: The figure above shows the three-dimensional aircraft with the wing configuration that was chosen in order to best satisfy the design requirements.

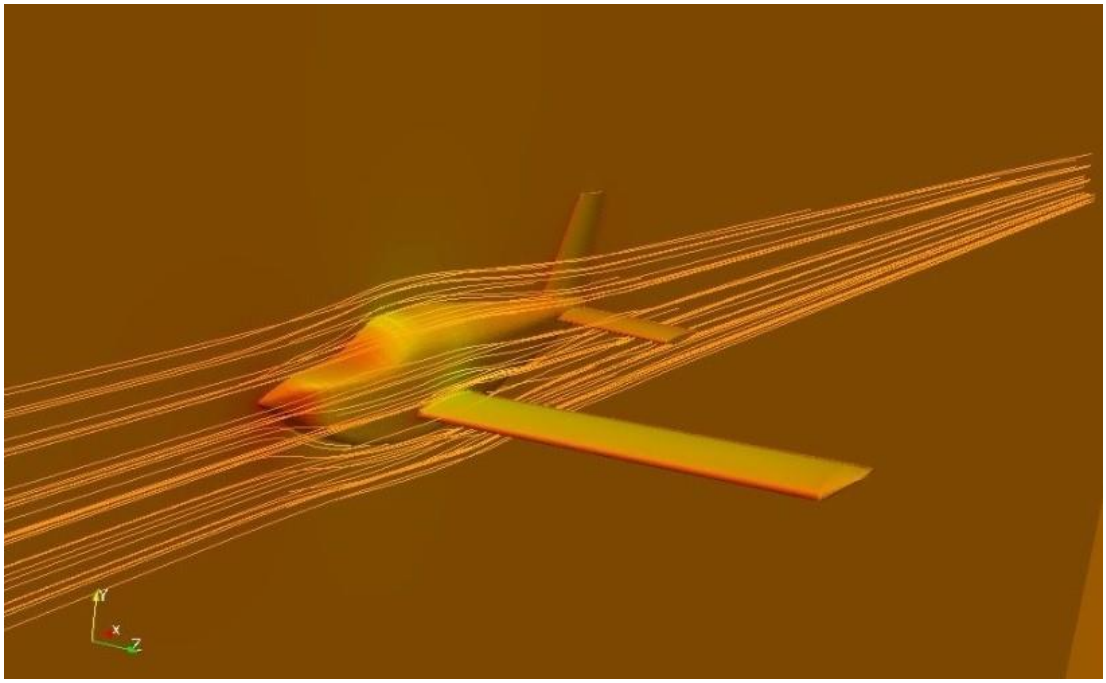

Figure 2.2: The image above depicts the 3D result of the analysis in OpenFoam. Some of the aircraft's flow lines are also shown, in order for us to understand the horizontal flight aerodynamic performance of the fuselage.

At this particular stage we gave the aircraft in its not-quite-final form and the overall plan that will allow us to estimate the aircraft's dimensions with the help of the LISA finite element program is now ready.

3) Finite element analysis

At this stage of the study, all structural parts of the aircraft will be measured using the finite element analysis of the LISA program. The design loads are calculated in a way that they are meeting its category's requirements of EASA and FAA.

The figures below are from the finite element analysis.

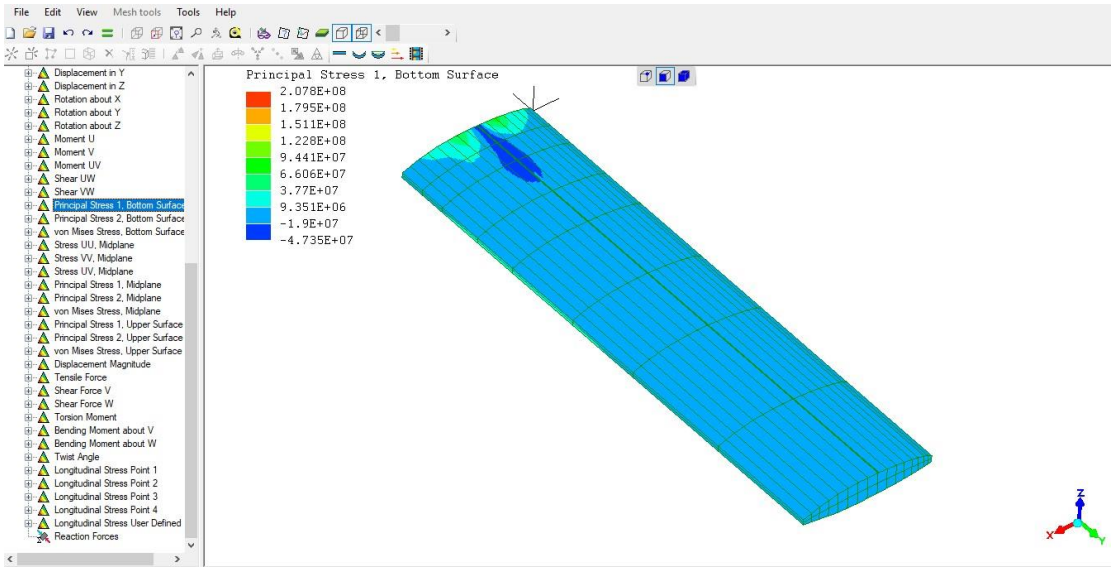

Figure 3.1: The figure above shows the stress forces exerted due to an 8g load during the flight.

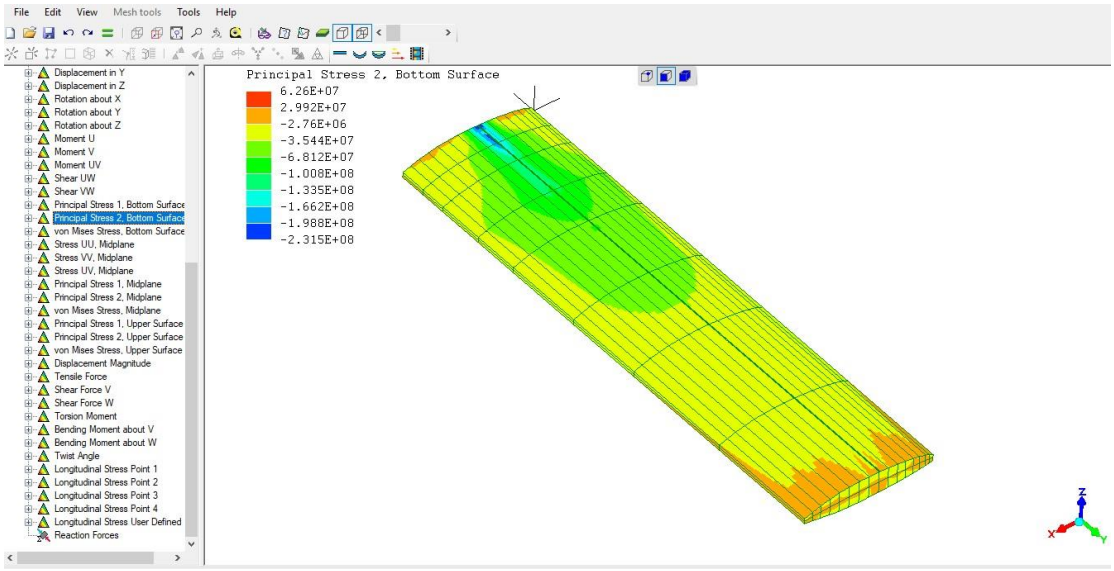

Figure 3.2: The figure above shows the stress forces exerted due to an 8g load during the flight.

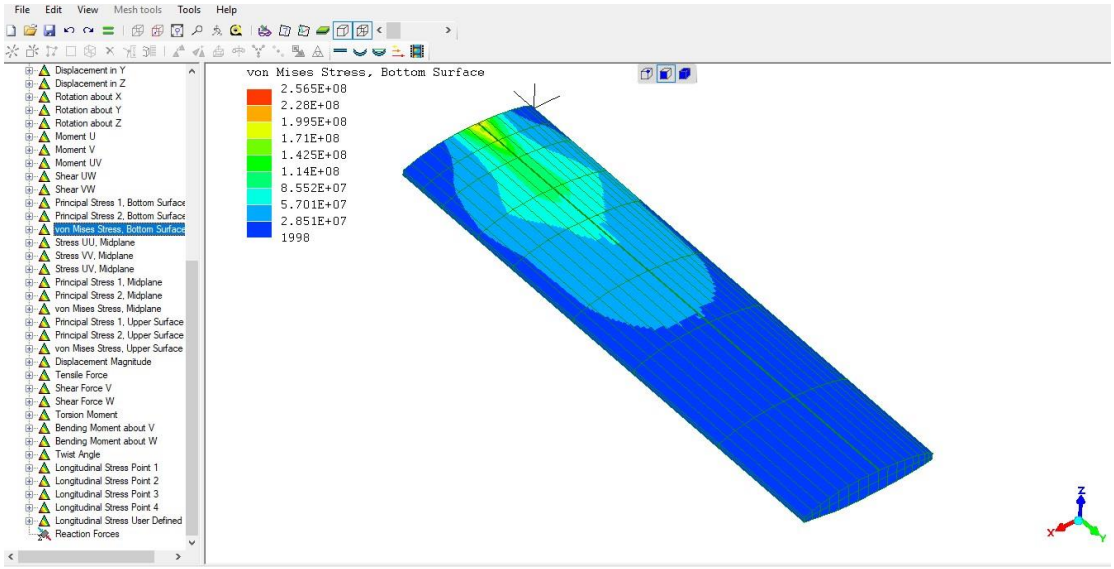

Figure 3.3: The figure above shows the stress forces exerted due to an 8g load during the flight.

It is easily observed that the wings' maximum expected load (limit load) is 8g.

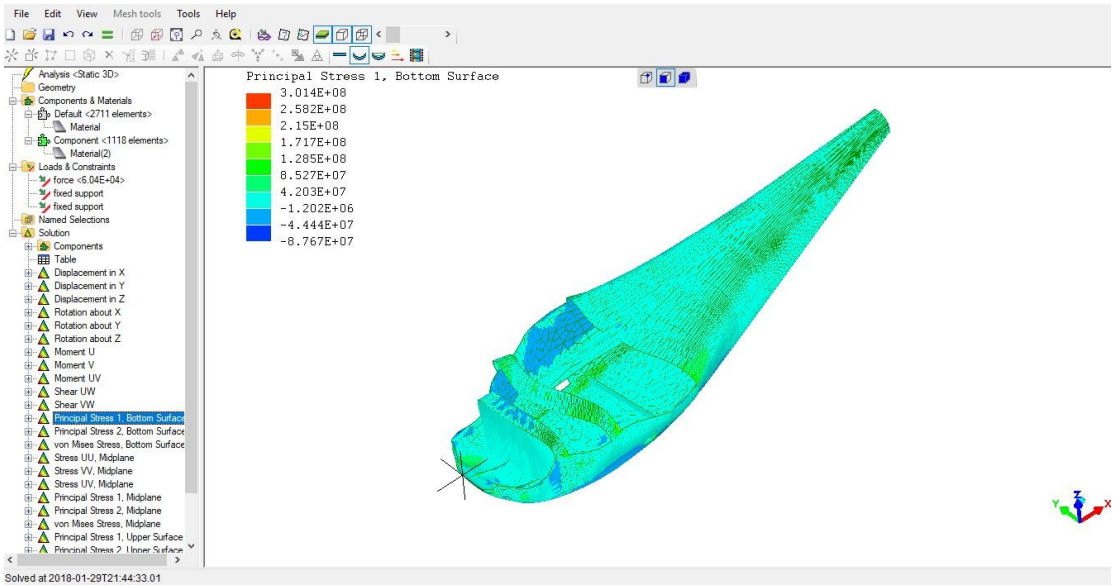

Figure 3.4: The figure above shows the stress forces exerted due to a 15g hard landing load.

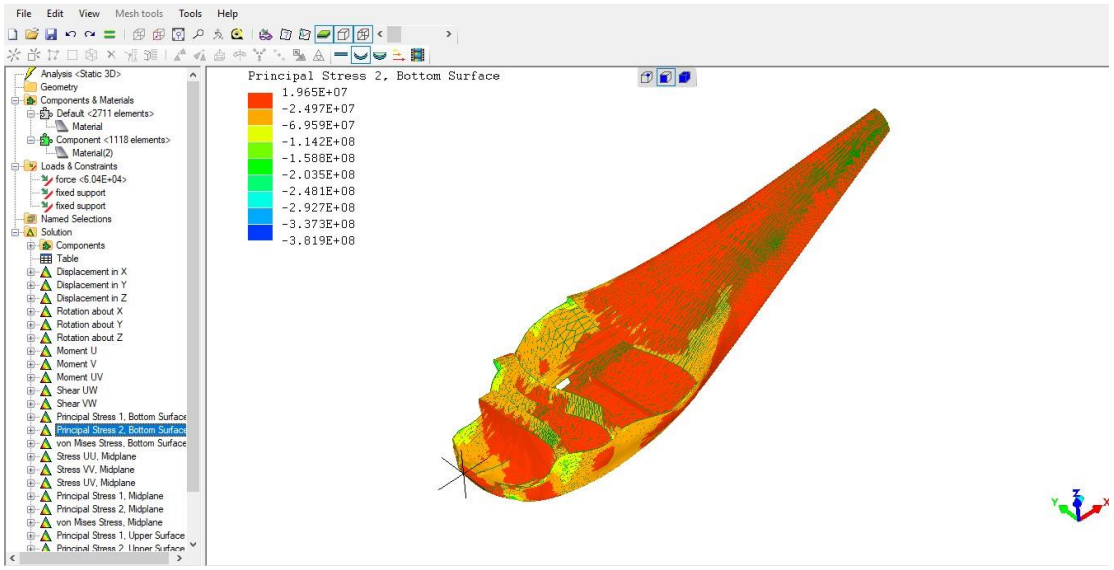

Figure 3.5: The figure above shows the stress forces exerted due to a 15g hard landing load.

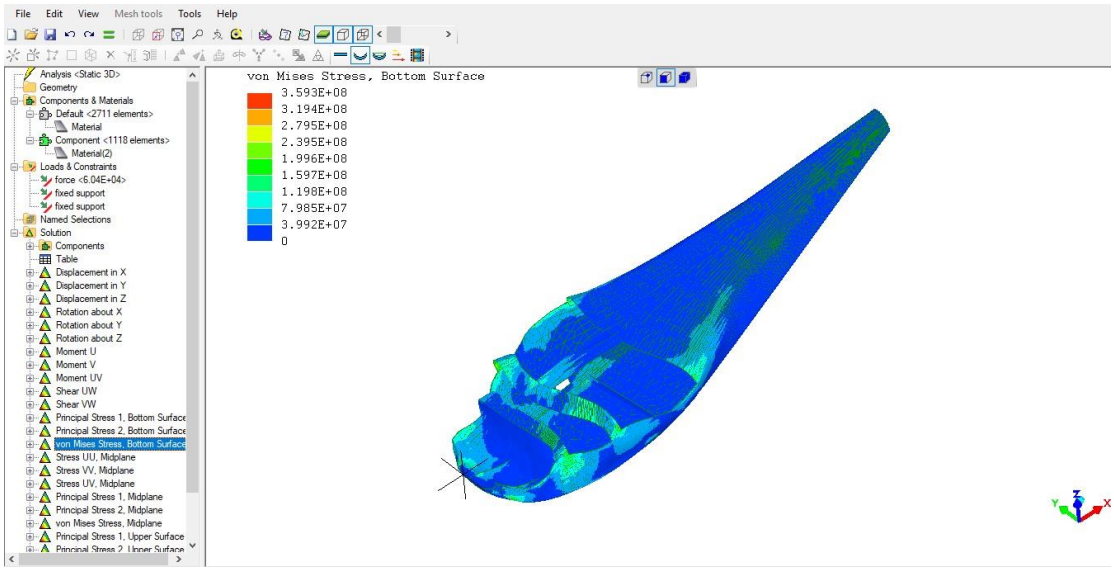

Figure 3.6: The figure above shows the stress forces exerted due to a 15g hard landing load.

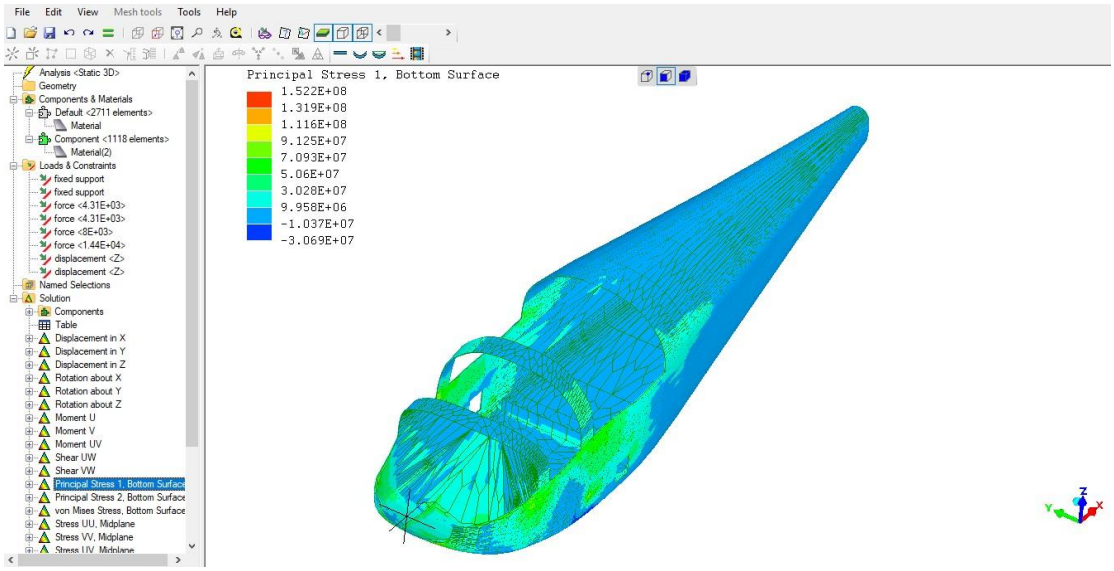

Figure 3.7: The figure above shows the stress forces exerted due to an 8g load during the flight.

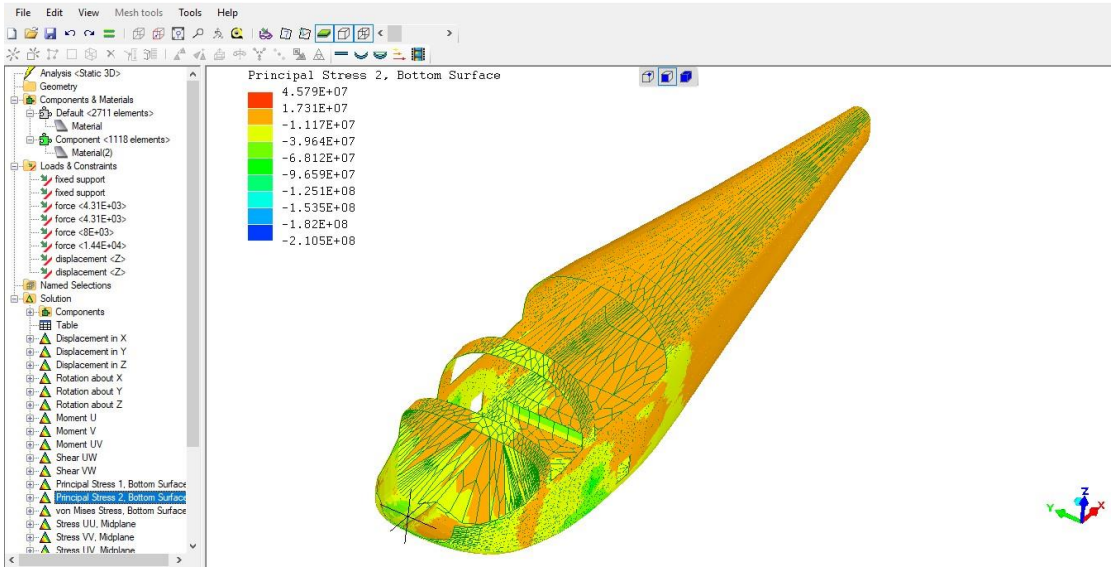

Figure 3.8: The figure above shows the stress forces exerted due to an 8g load during the flight and a propeller load with a safety factor of 5.

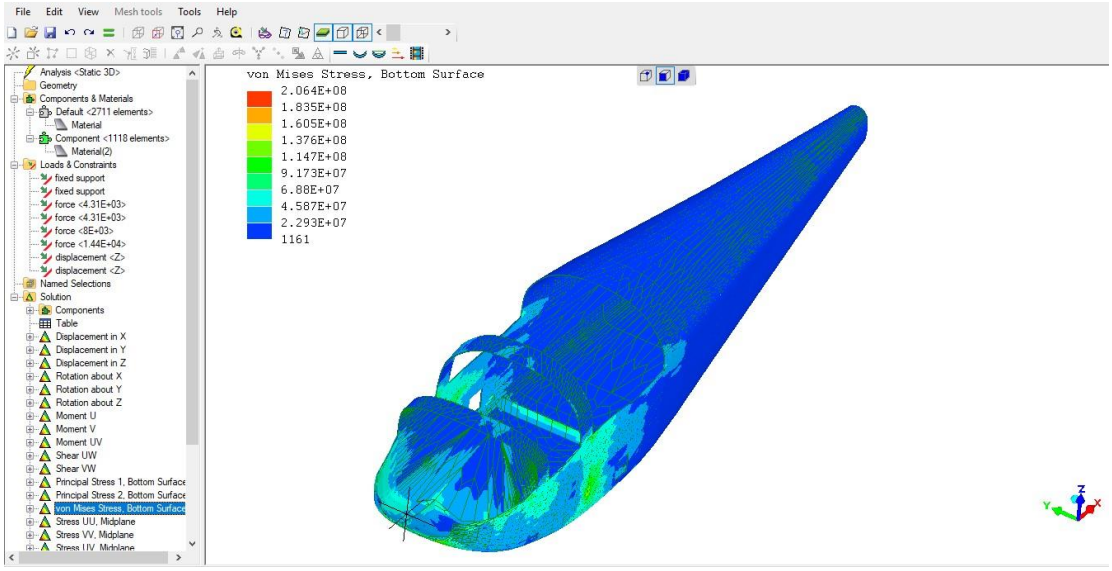

Figure 3.9: The figure above shows the stress forces exerted due to an 8g load during the flight and a propeller load with a safety factor of 5.

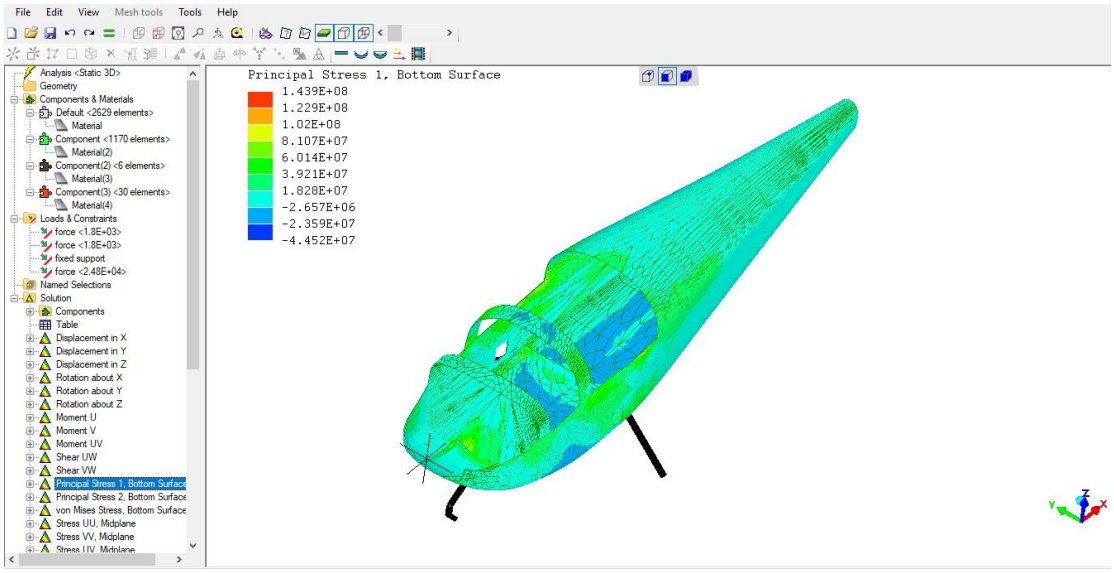

Figure 3.10: The figure above shows the stress forces exerted due to a 6g load during landing.

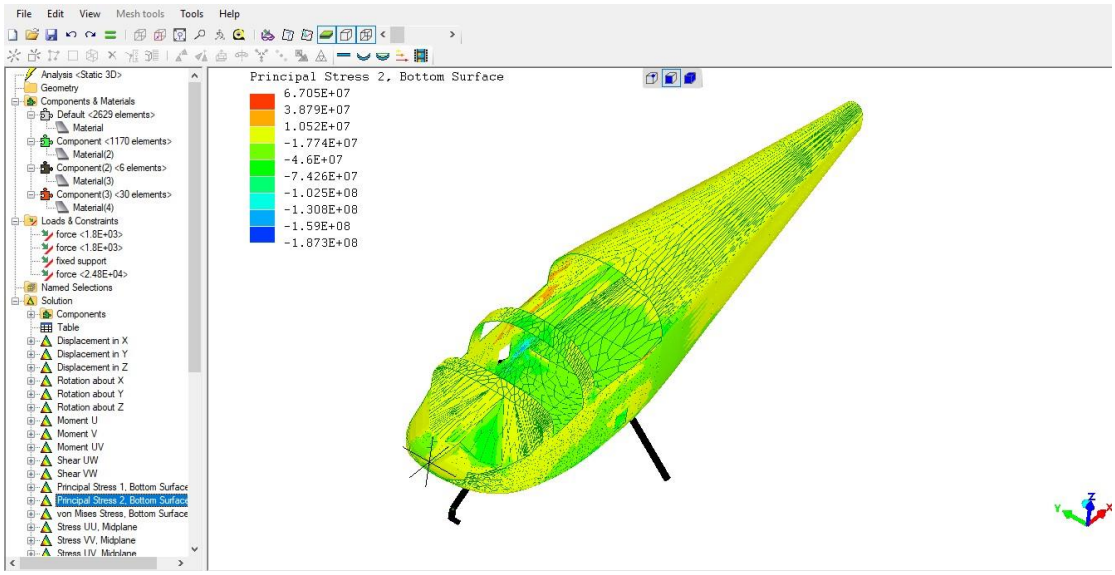

Figure 3.11: The figure above shows the stress forces exerted due to a 6g load during landing.

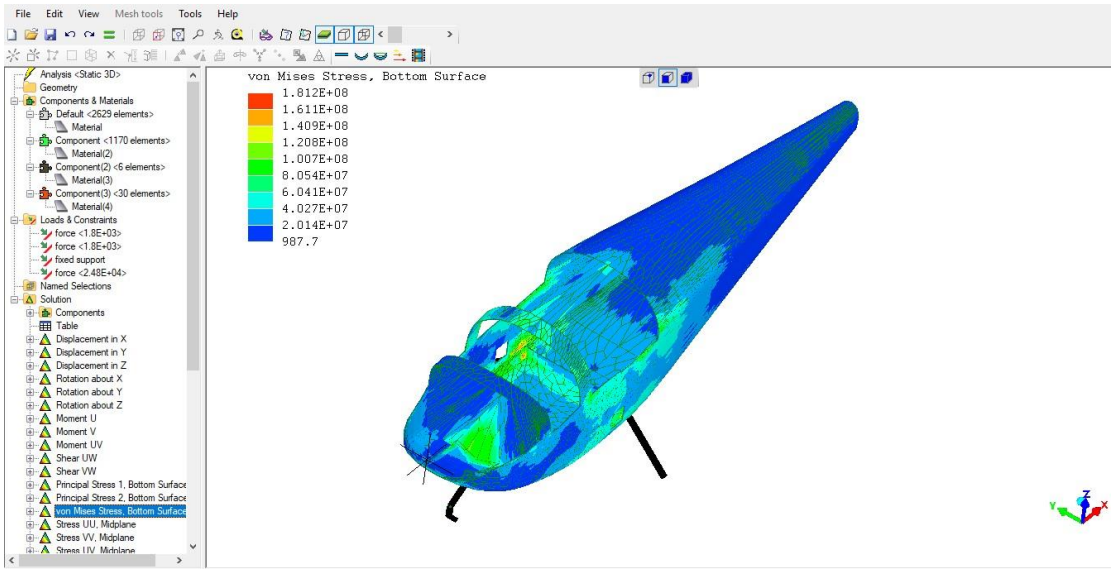

Figure 3.12: The figure above shows the stress forces exerted due to a 6g load during landing.

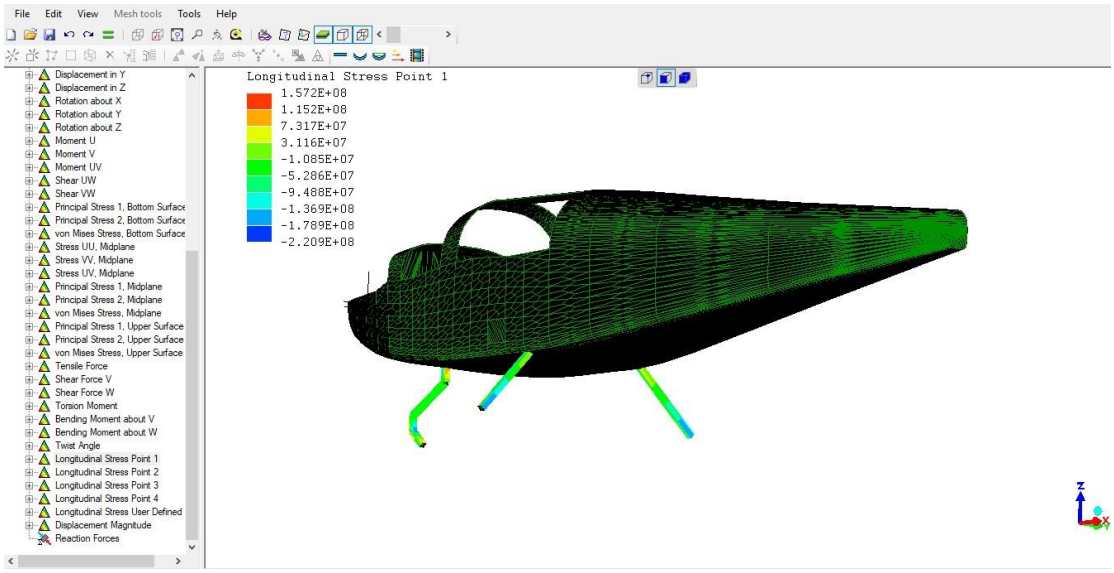

Figure 3.13: The figure above shows the stress forces exerted due to a 6g load during landing.

Comments:

The wings and fuselage are durable for stress forces exerted due to an 8g load, the fuselage durable enough to withstand a collision load of 15g. Finally, the engine mounts are durable enough to withstand a propeller load with a safety factor of 5. The landing system has a load-bearing capacity of up to 6g during landing.

During collision the fuselage remains within the elastic region up to 15g. It is of a satisfactory size and so the design of the aircraft can continue. In the next chapter, the behavior of the fuselage frame will be studied with the help of the Code_Aster program.

4) Aircraft's Flight stability analysis

The aircraft's building materials as well as the method and the cross sections have already been selected and it is tested that they meet the requirements of the present study. From this data the center of gravity and the moments of inertia were calculated. The vlm program was programmed according to these elements, in order for us to perfect the aircraft's design by creating a stable and tractable aircraft.

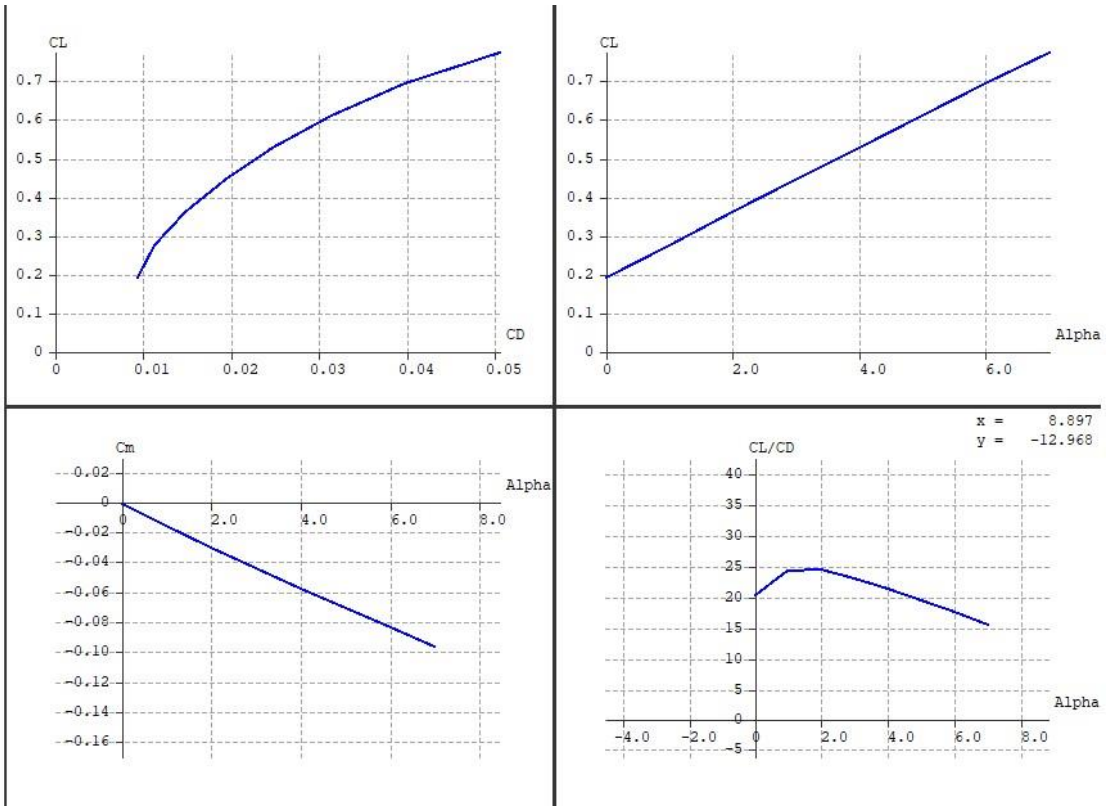

Figure 4.1: The aircraft is statically stable and Cm = 0 for 0 ° AOA. For 0 ° AOA, Cl > 0, the plane is flying. It is noticed that the lift to drag ratio (glide ratio) is very satisfactory, for which the very small drag of the aircraft is responsible.

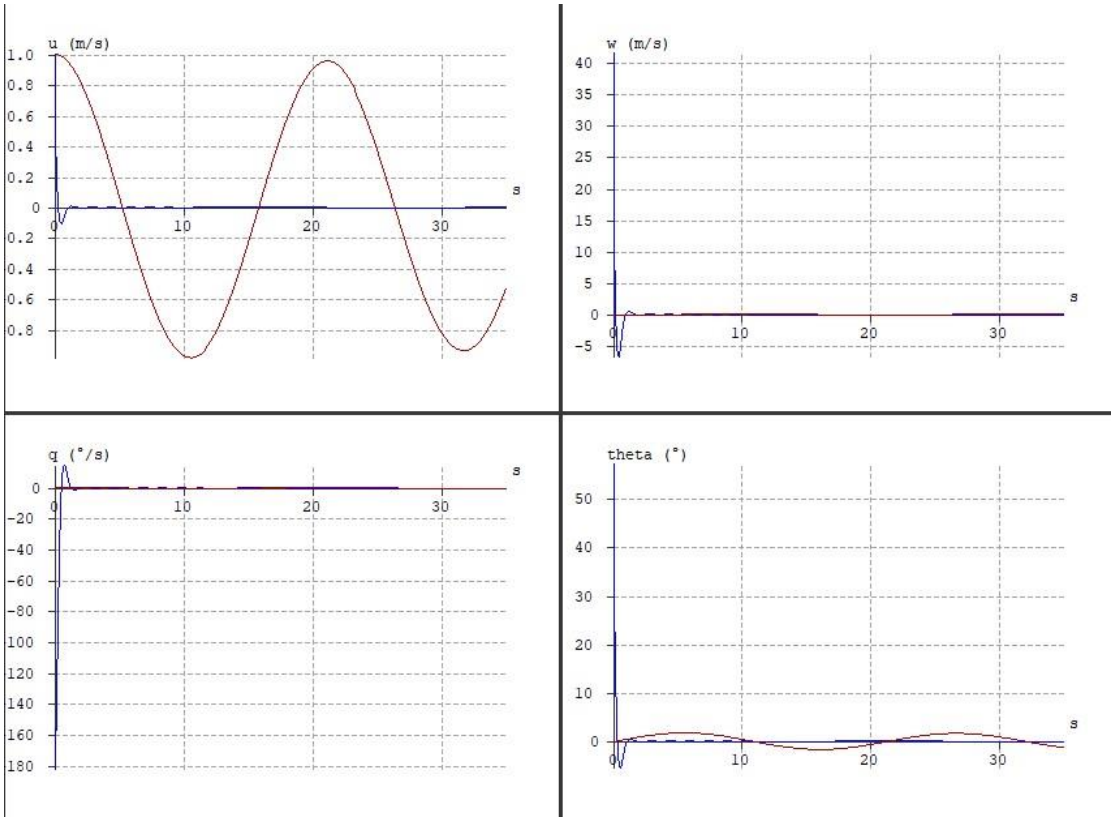

Figure 4.2: longitudinal

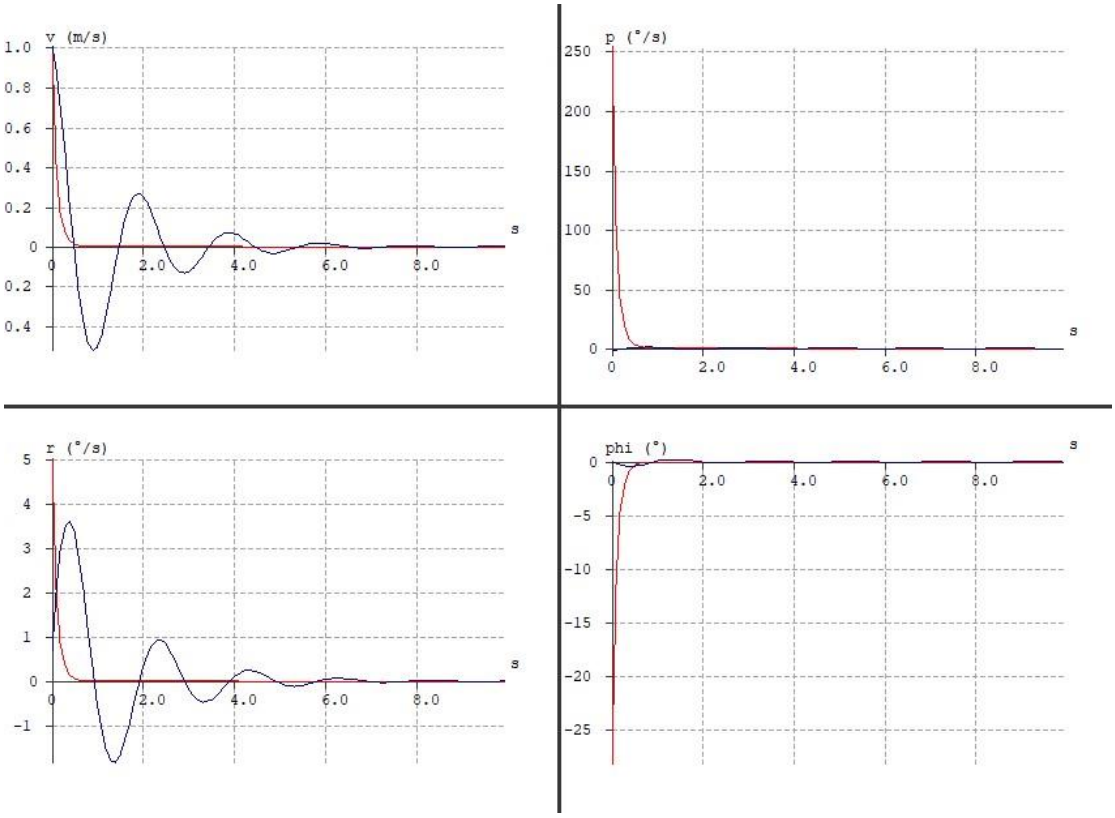

Figure 4.3: lateral

Comment:

The aircraft is also dynamically stable. The center of gravity's initial estimate was almost identical to the actual one, yet another finite analysis was done, the aircraft is meeting the design goals, so the study can continue.

5) CFD analysis in OpenFoam

In the figures below we see the results from the analysis performed in OpenFoam. In order for us to ensure the safety and performance of the aircraft all possible flight and speed combinations were studied. From this high-precision analysis the flight program that follows was also created. Also, the characteristics of the propeller (power, speed range, diameter, number of blades and pitch) were selected having taken into consideration the drag data of the analysis as well as the flight speed.

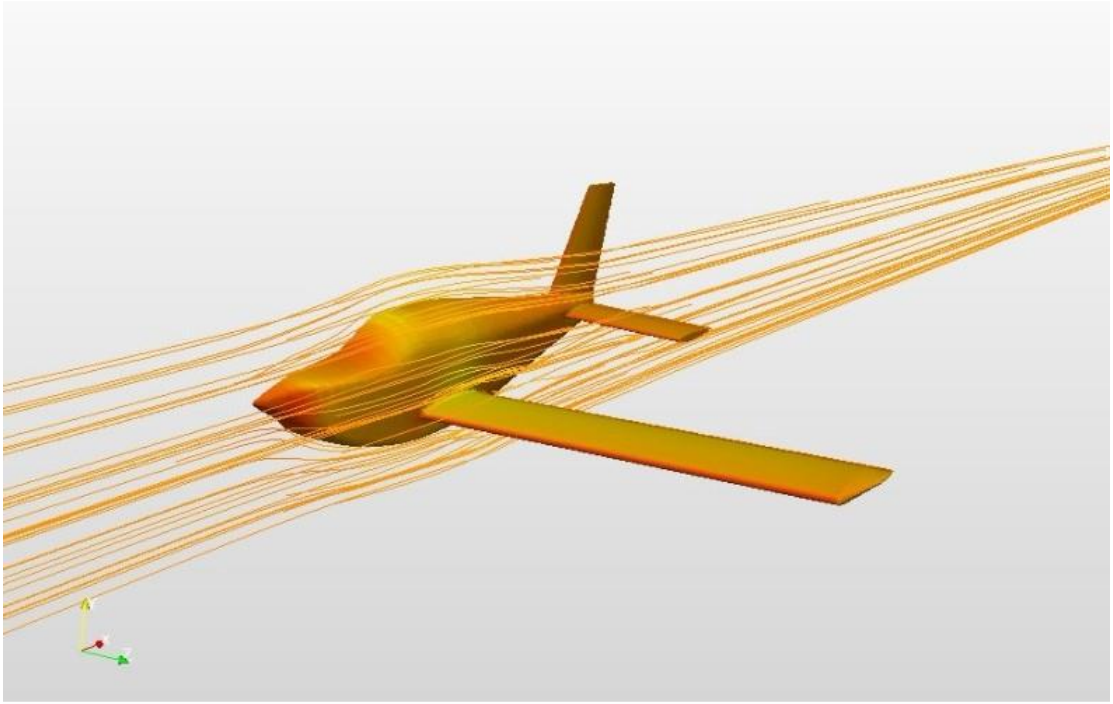

Figure 5.1: Result of the aerodynamic analysis for a flight at maximum speed

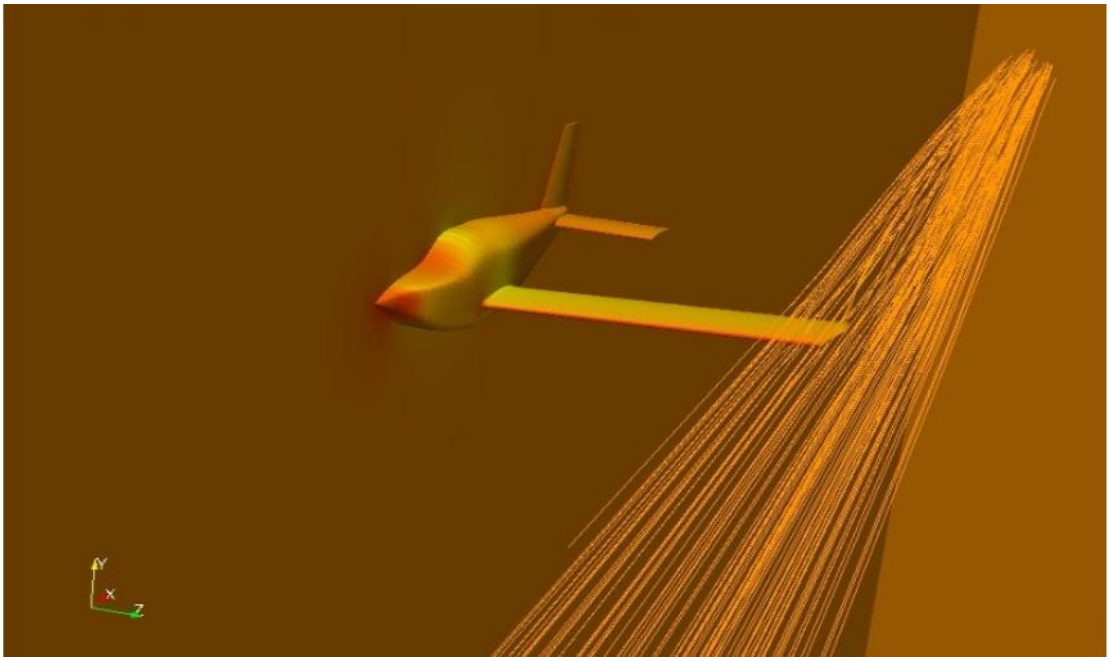

Figure 5.2: Result of the aerodynamic analysis for a flight at maximum speed

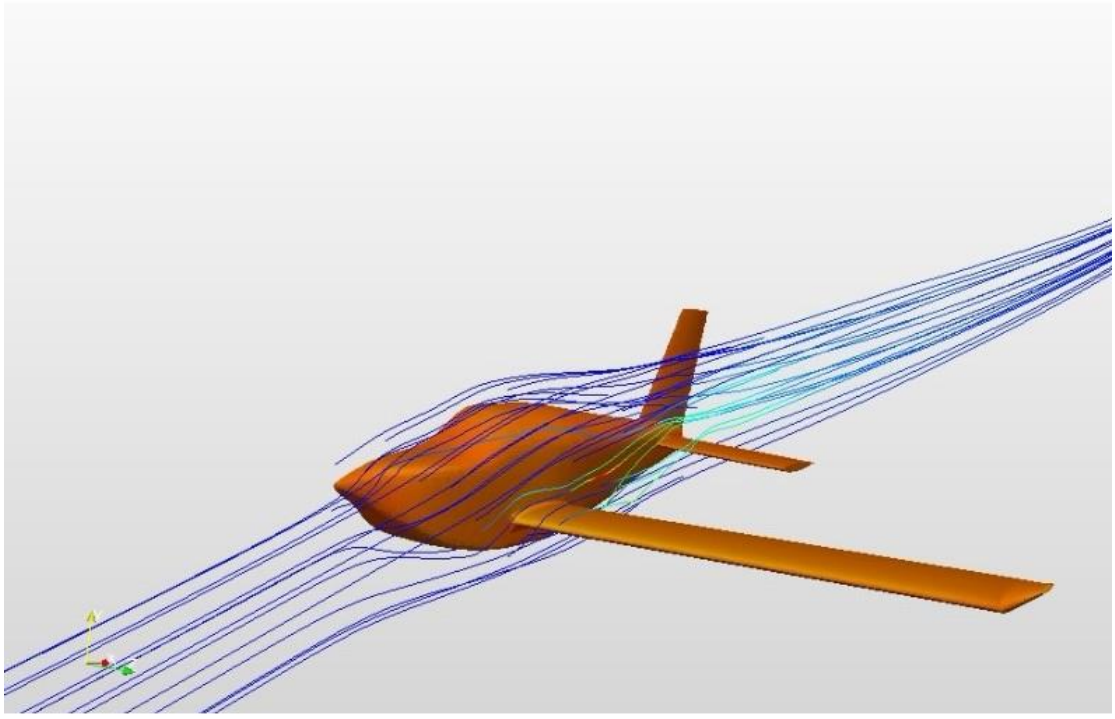

Figure 5.3: Result of the aerodynamic analysis for a flight at approach speed. At this point it was studied whether the main wing vortices negatively affect the elevator's performance to an extent that it becomes dangerous for the flight's safety.

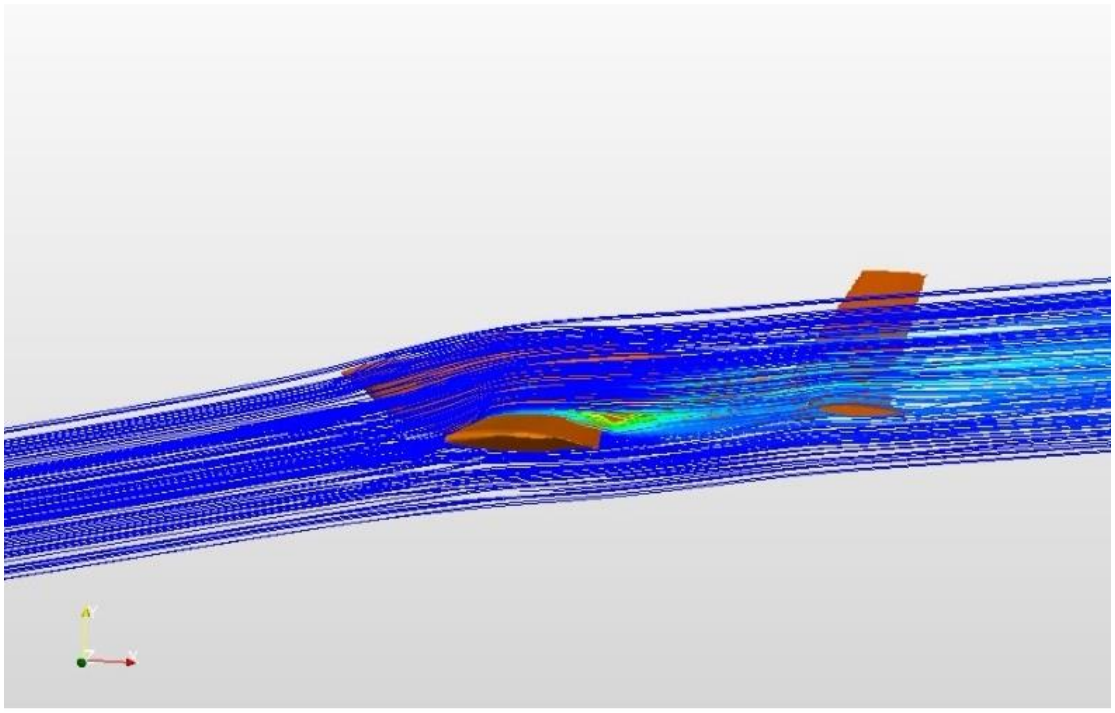

Figure 5.4: Result of the aerodynamic analysis for a flight close to stall speed. At this point it was studied whether the main wing vortices negatively affect the elevator's performance to an extent that it becomes dangerous for the flight's safety. From this angle the loss support vortexes in the wing root are also visible. Should we have an irrotational flow round the endpoint, the twist (washout) is satisfactory.

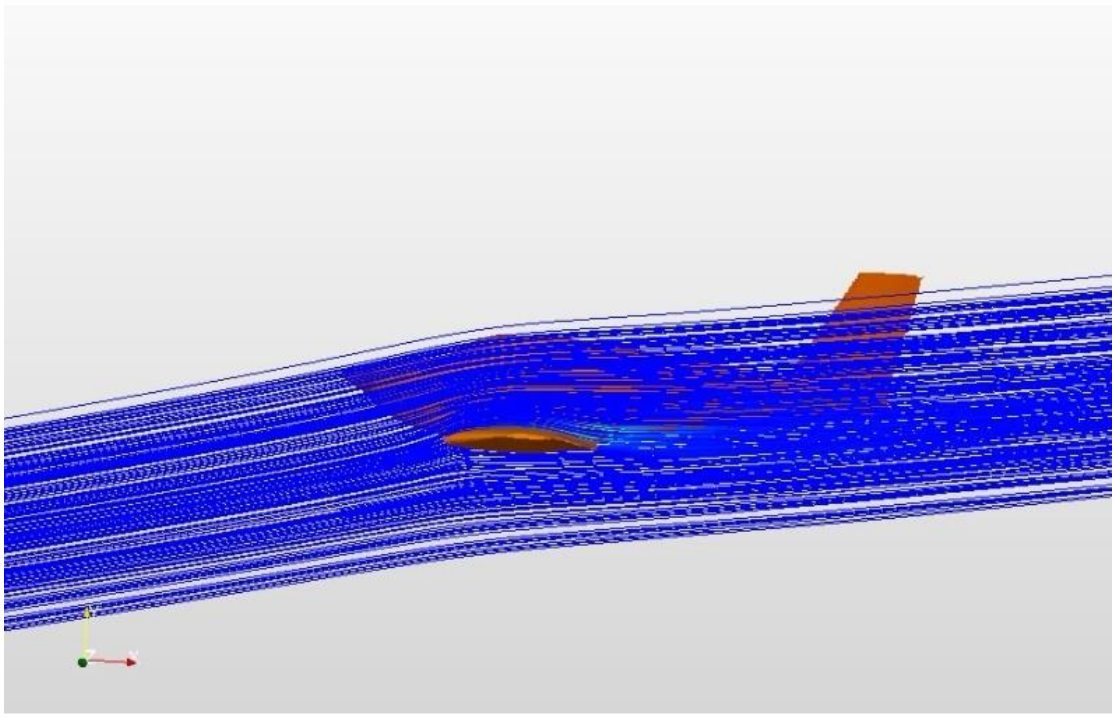

Figure 5.5: Result of the aerodynamic analysis for a flight close to stall speed. We have an irrotational flow round the endpoint, the twist (washout) is satisfactory.

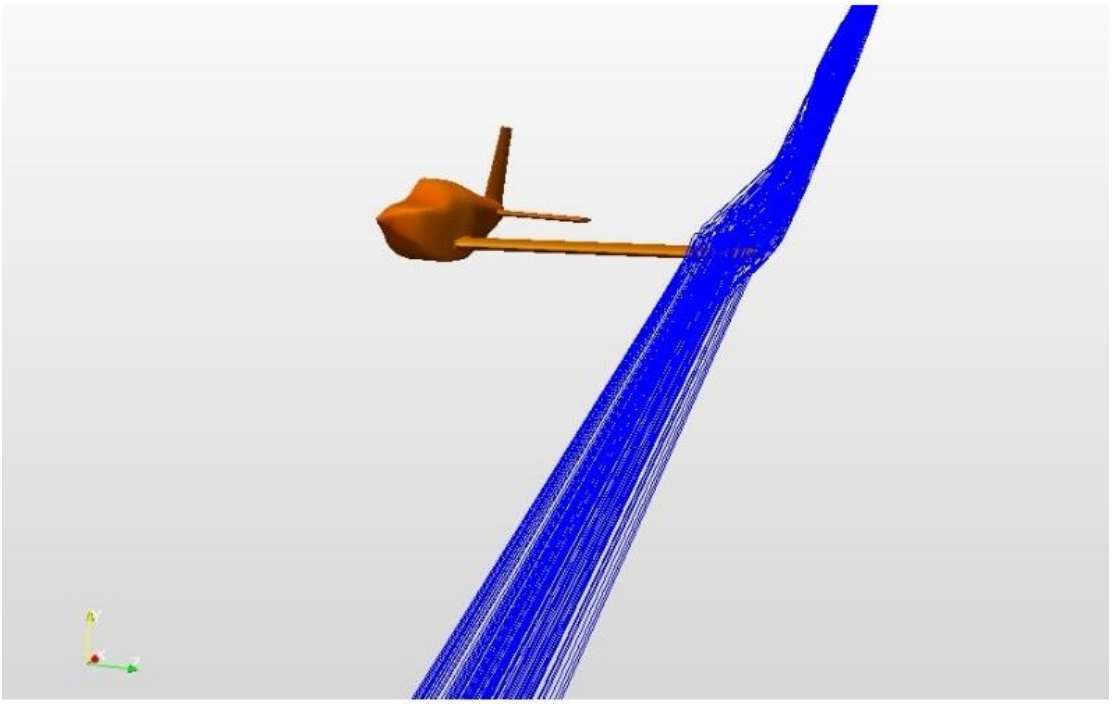

Figure 5.6: Result of the aerodynamic analysis for a flight close to stall speed. At this point the correct performance of the wingtip was studied. It was designed in such way that the airflow produced by the pressure difference between the lower and upper surface of the flap creates a vortex (known as wingtip vortices), though one that will not hit the top of the flap. This resulted to a higher buoyancy coefficient, lower stall speed and a better behavior as the ailerons receive air without vortices.

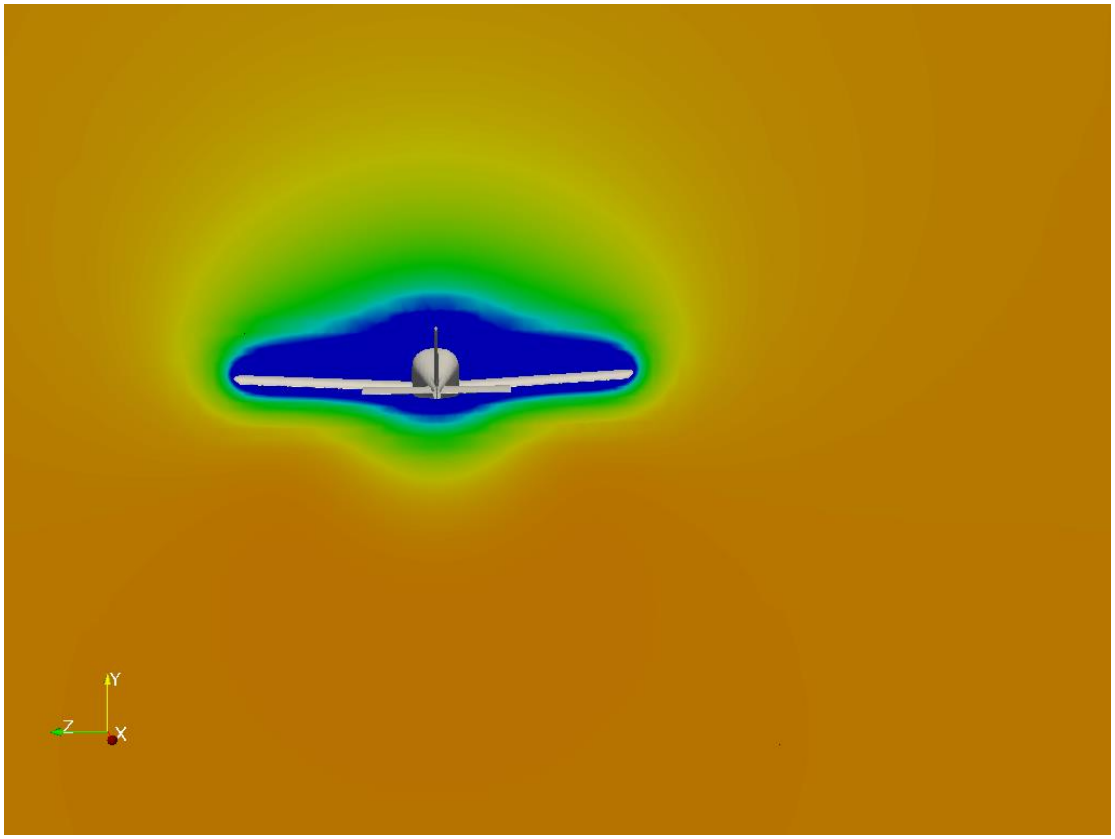

Figure 5.7: Pressures around the aircraft at cruise speeds.

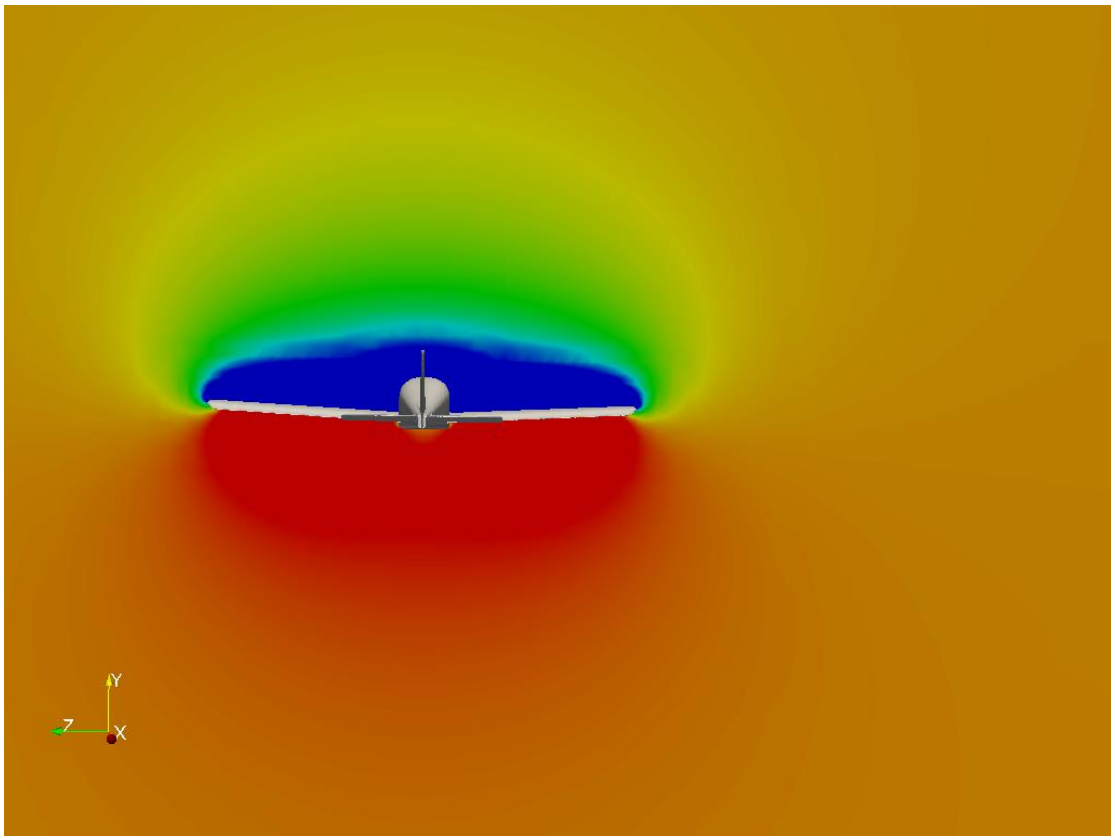

Figure 5.8: Pressures around the aircraft at approach speeds.

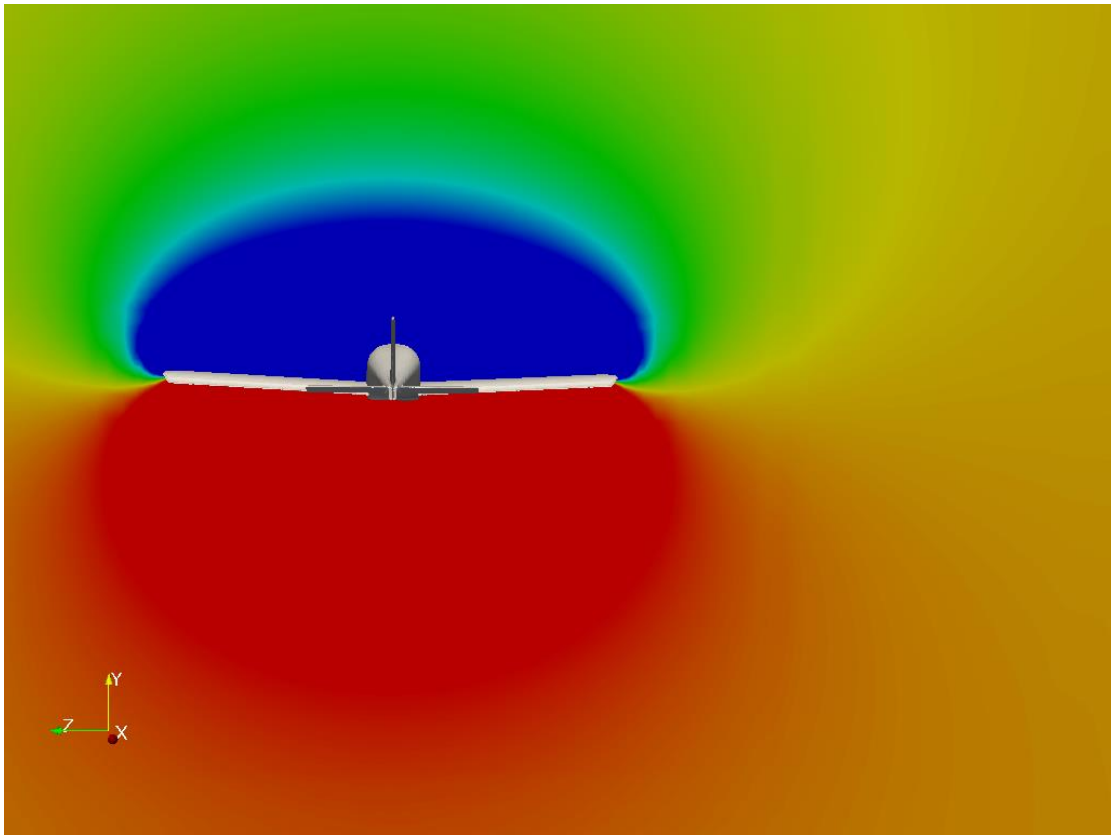

Figure 5.9 Pressures around the aircraft at take-off speeds.

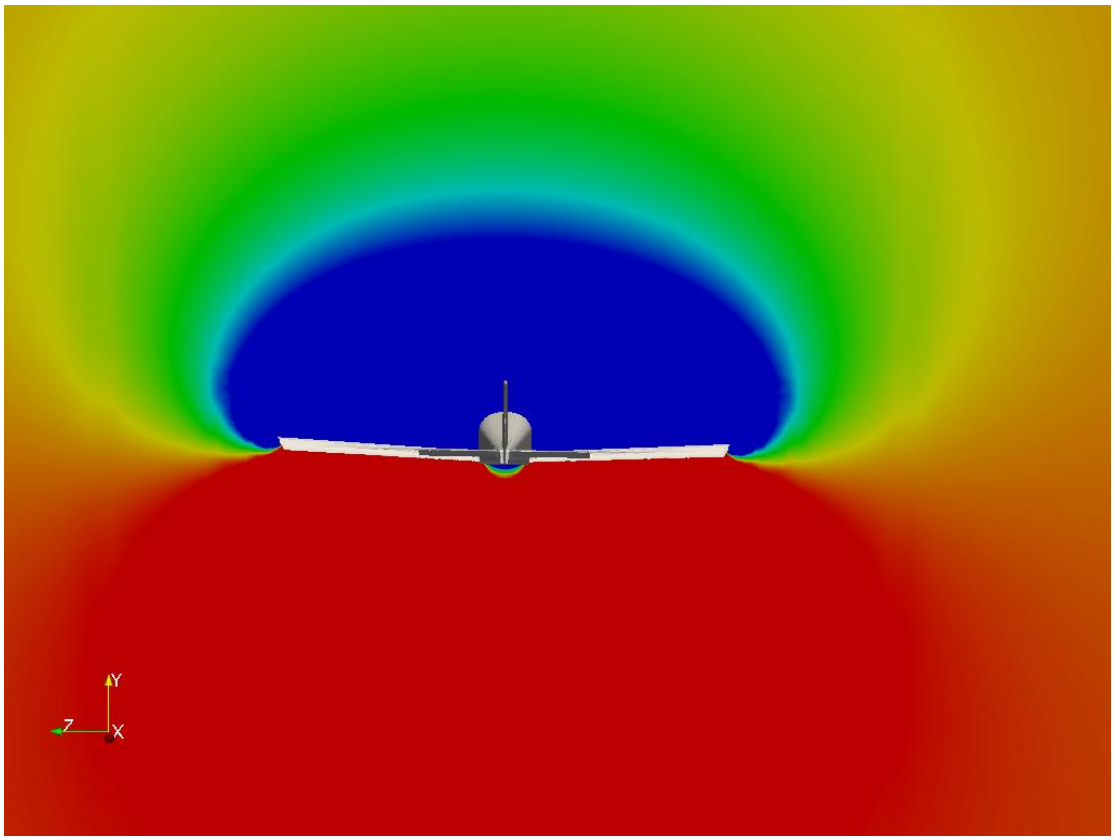

Figure 5.10: Pressures around the aircraft at final approach speeds.

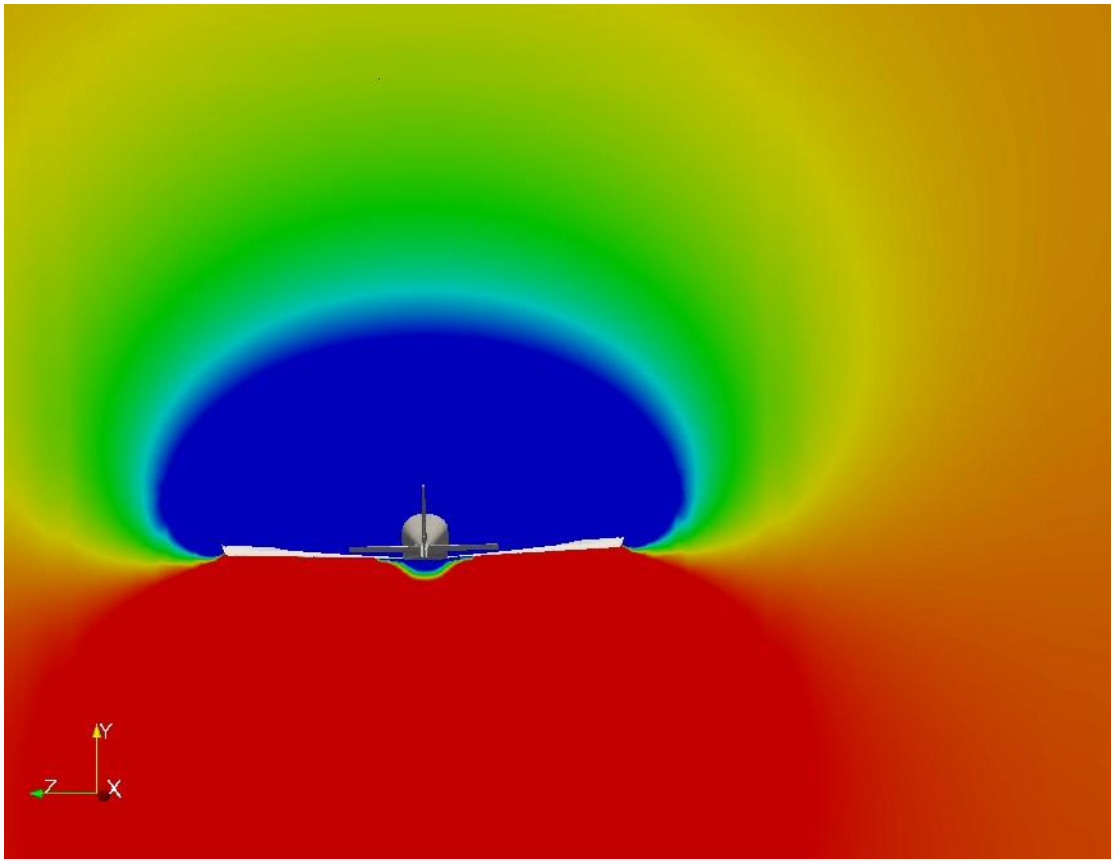

Figure 5.11: Pressures around the aircraft at speeds just before stall with fully extended flaps.

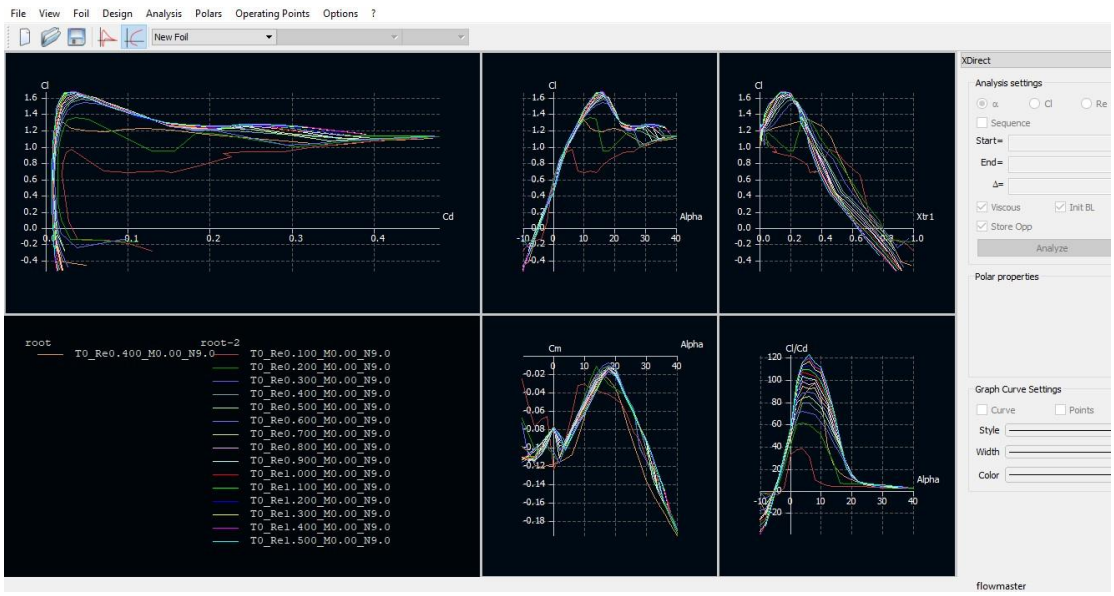

Figure 5.12: Graphs of buoyancy and drag created by the vortex lattice method (jblade) program initially used for the propeller's design. At this point a two-dimensional analysis of different airfoils is made in order for us to select the most appropriate combination that will form the propeller flap.

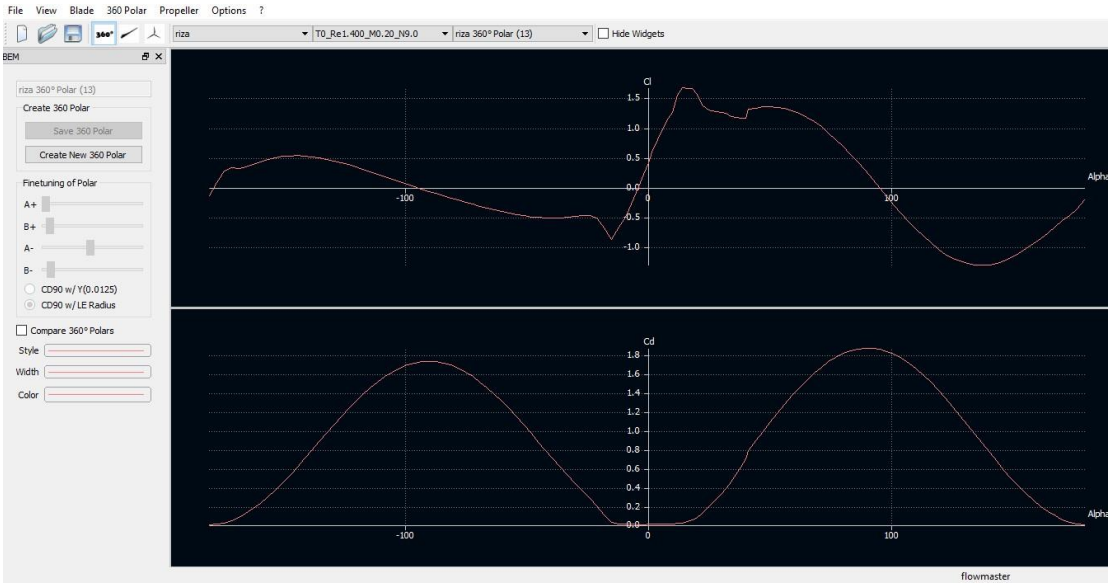

Figure 5.13: Graphs of buoyancy and drag created by the vortex lattice method (jblade) program initially used for the propeller's design. At this point a 360 degrees analysis of the airfoils is made (for convenience, we only show one). Then, with the help of the Prandtl numbers they will eventually be shown in a three-dimensional flap.

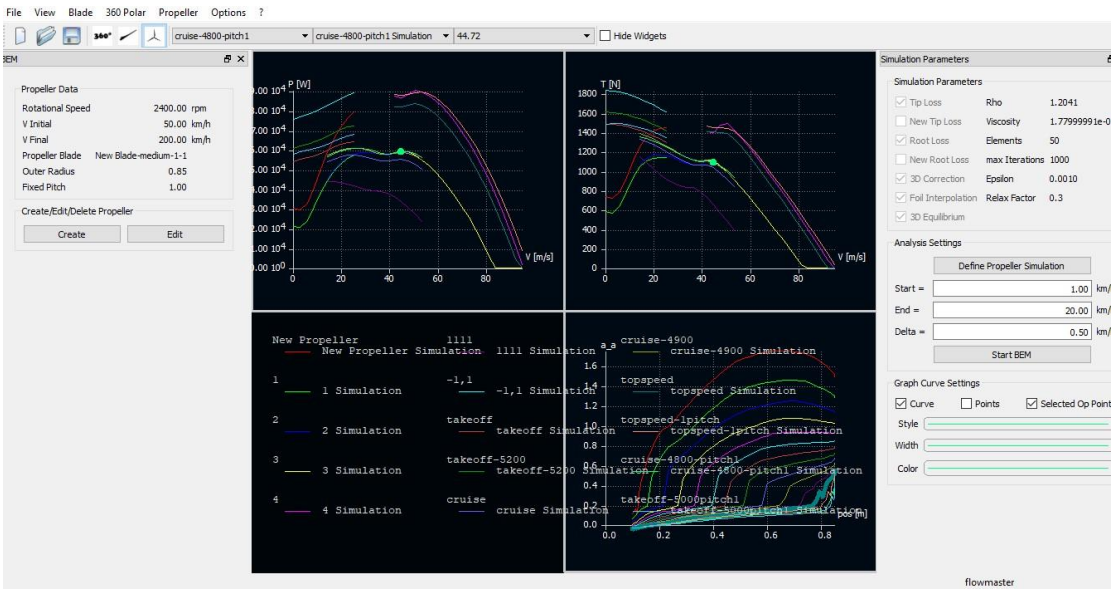

Figure 5.14: Propeller analysis using the vortex lattice method program. We have all the necessary data to make a choice. After running several tests in the three-dimensional design, the designer concluded that the best propeller was the one with the characteristics above (we show only the final test and not all of them, for convenience). Moreover, below we see the analysis results using OpenFoam.

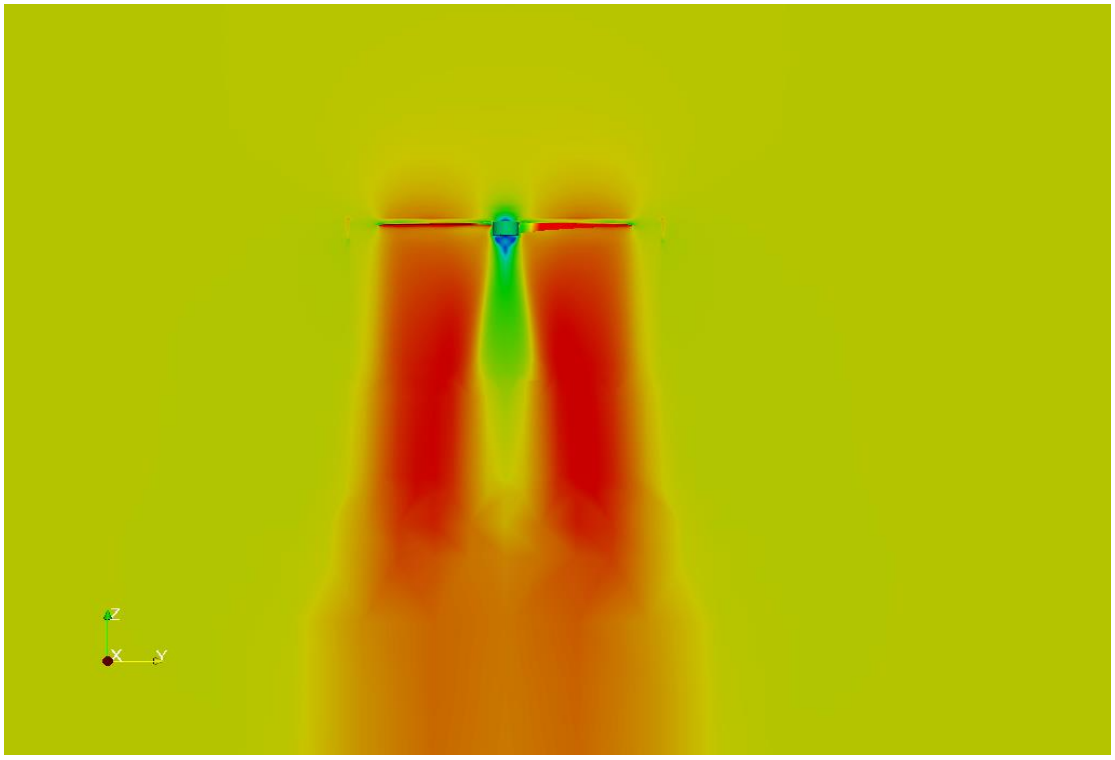

Figure 5.15: Propeller analysis at climb speed with the help of OpenFoam. The figure above shows the speeds around the propeller.

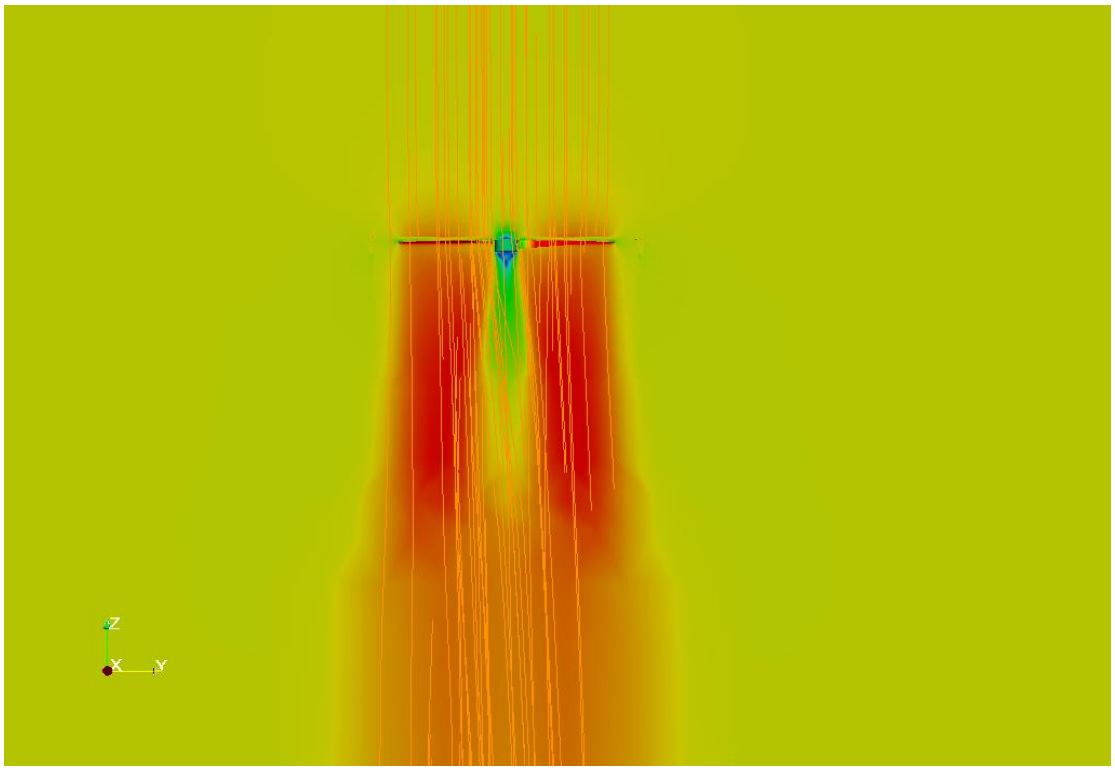

Figure 5.16: Propeller analysis at climb speed with the help of OpenFoam. The figure above shows the speeds around the propeller, as well as the flow lines that indicate the propeller's "pulling" direction.

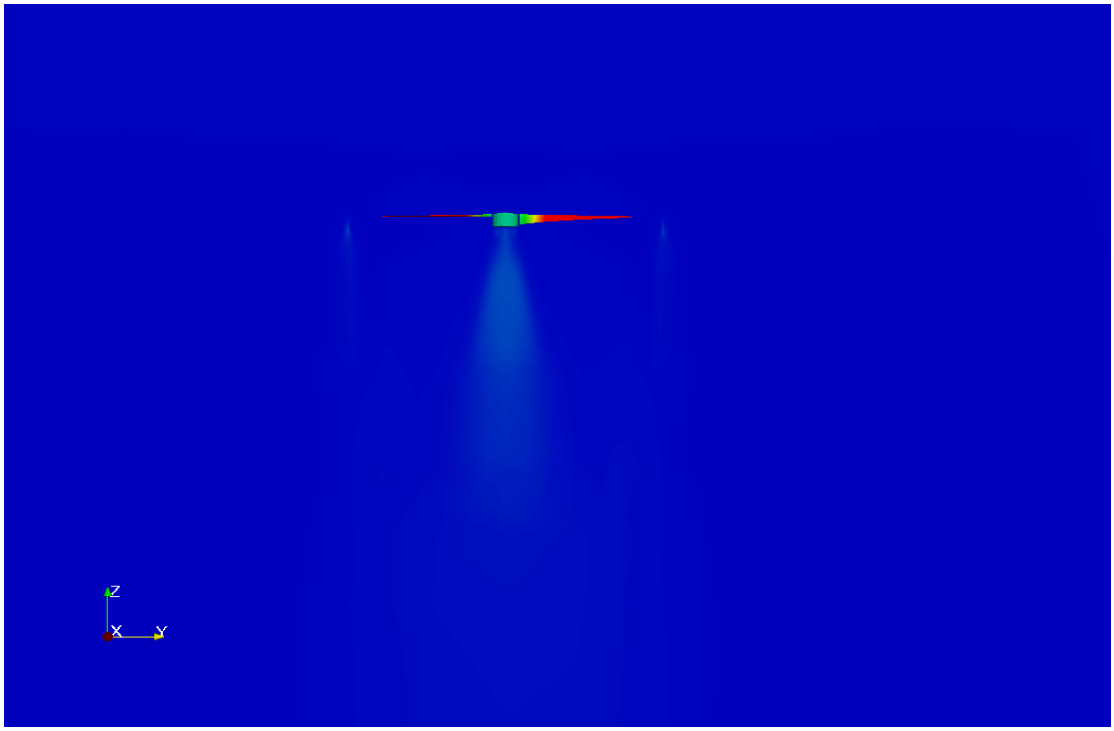

Figure 5.17: Propeller analysis at climb speed with the help of OpenFoam. The figure above shows the speeds around the propeller, as well as the flow lines that indicate the propeller's "pulling" direction. The flow is irrotational due to the high performance coefficient of the propeller. This propeller is indeed ideal for this aircraft.

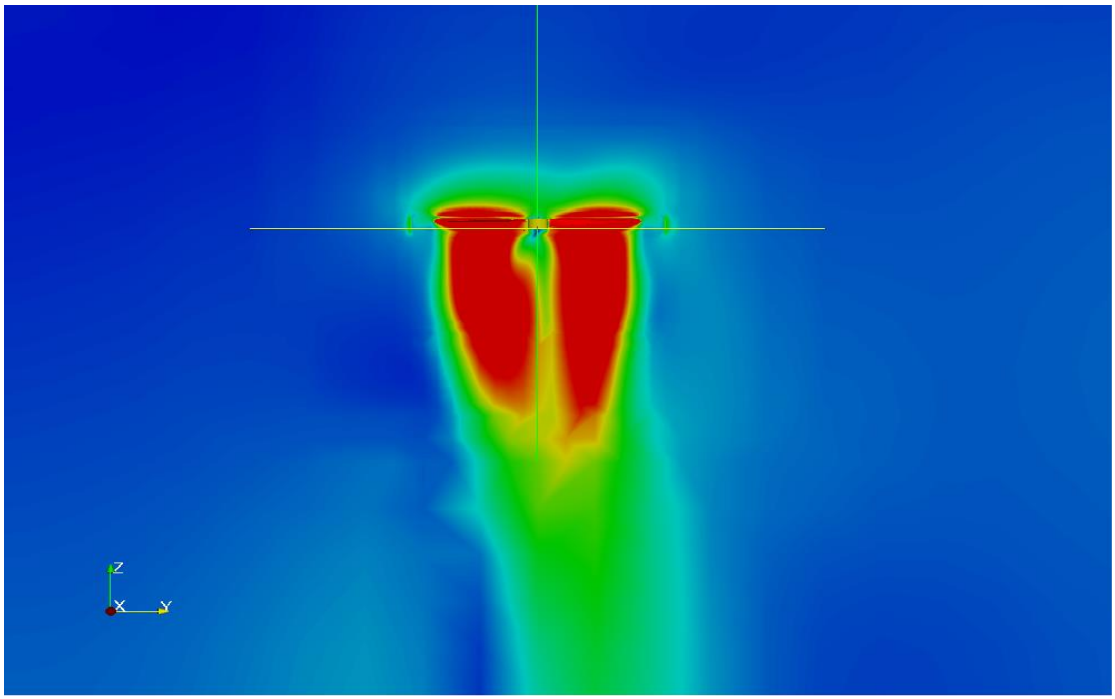

Figure 5.18: Propeller analysis at maximum ground power with the help of OpenFoam. The figure above shows the speed profile around the propeller.

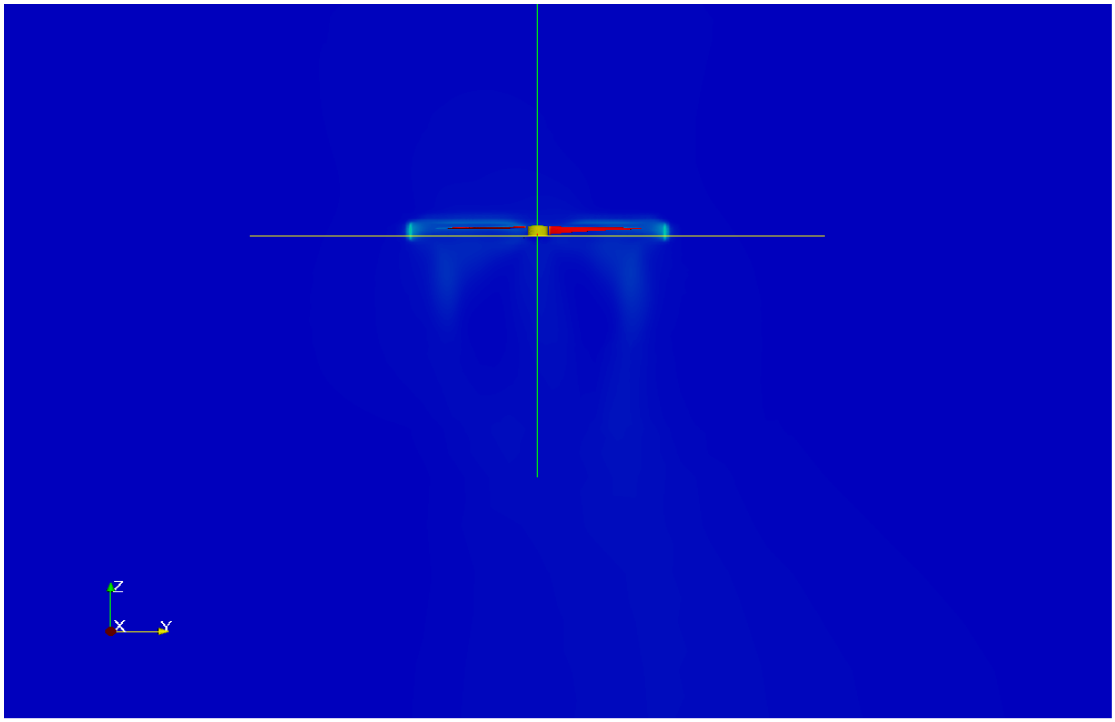

Figure 5.19: Propeller analysis at maximum ground power with the help of OpenFoam. The figure above shows the vortices around the propeller.

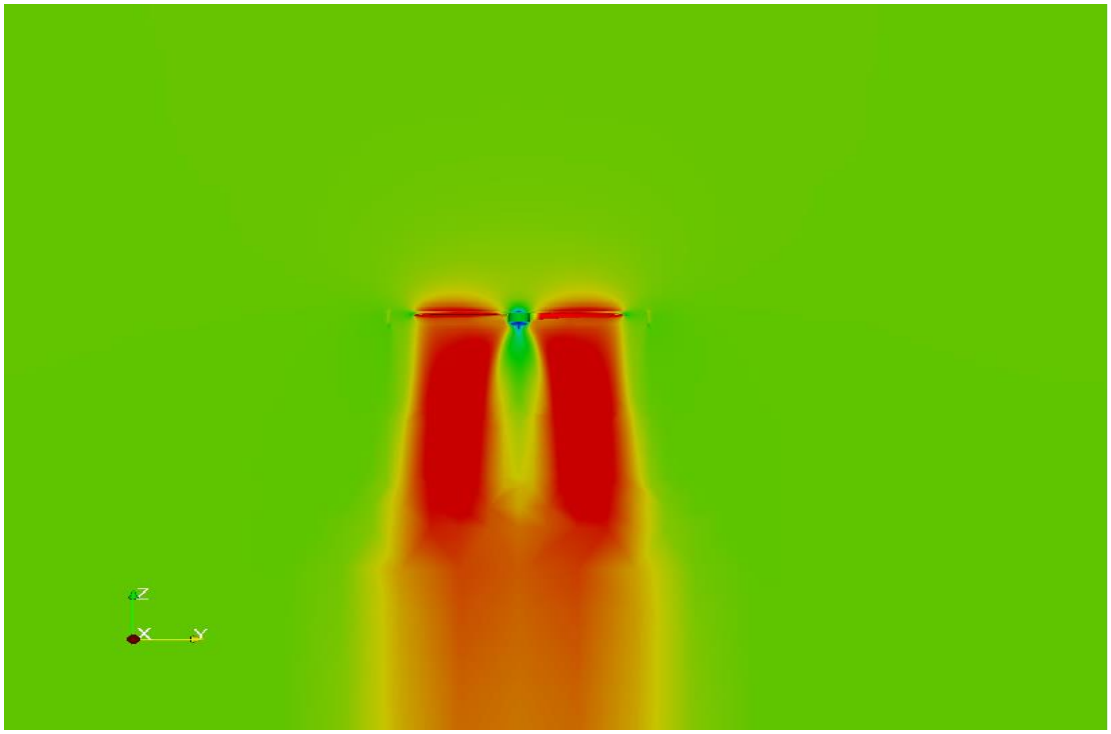

Figure 5.20: Propeller analysis at take-off speed with the help of OpenFoam. The figure above shows the speed profile around the propeller.

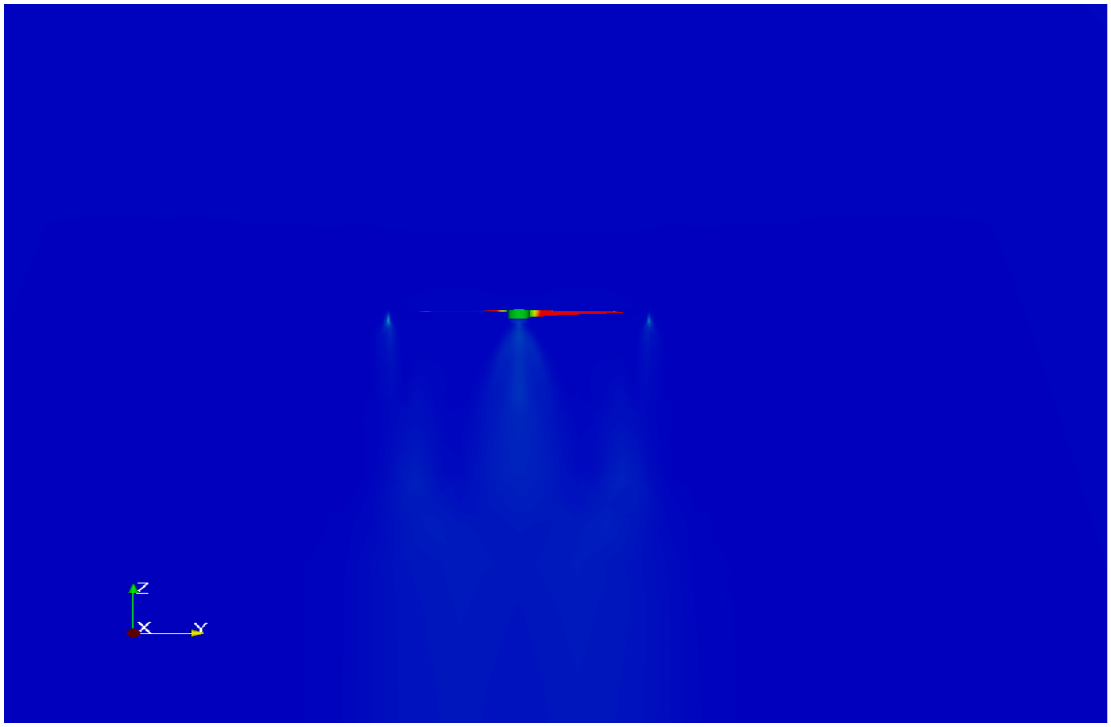

Figure 5.21: Propeller analysis at take-off speed with the help of OpenFoam. The figure above shows the vortices around the propeller.

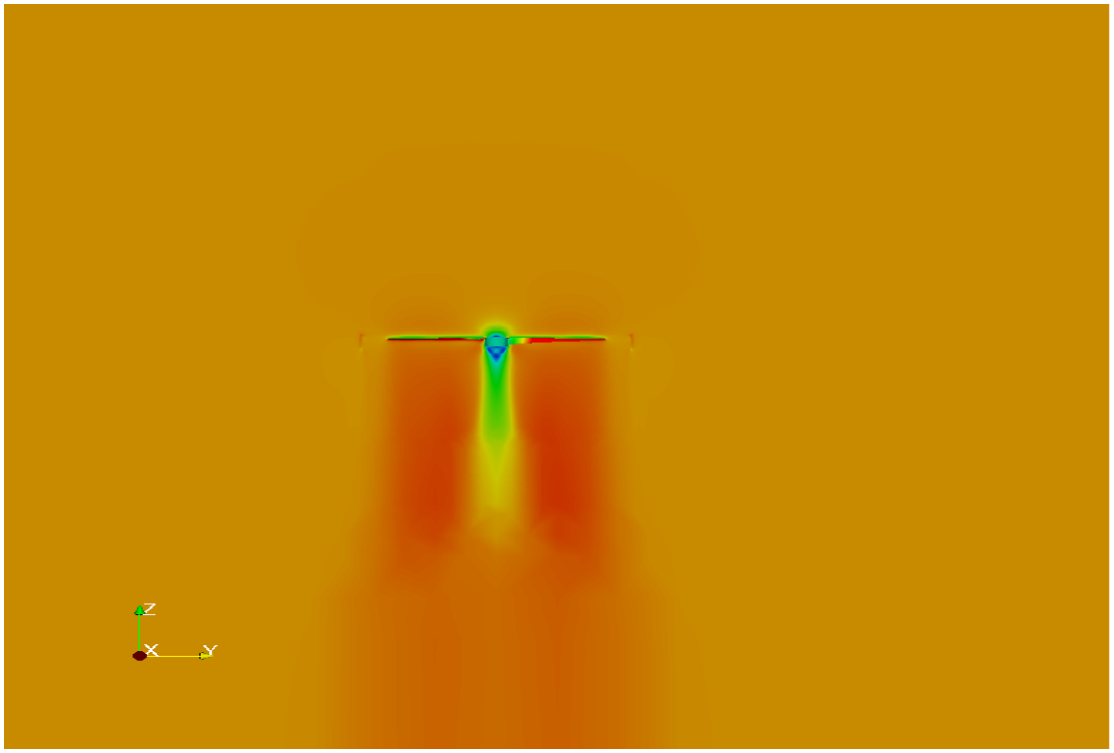

Figure 5.22: Propeller analysis at maximum speed with the help of OpenFoam. The figure above shows the speed profile around the propeller.

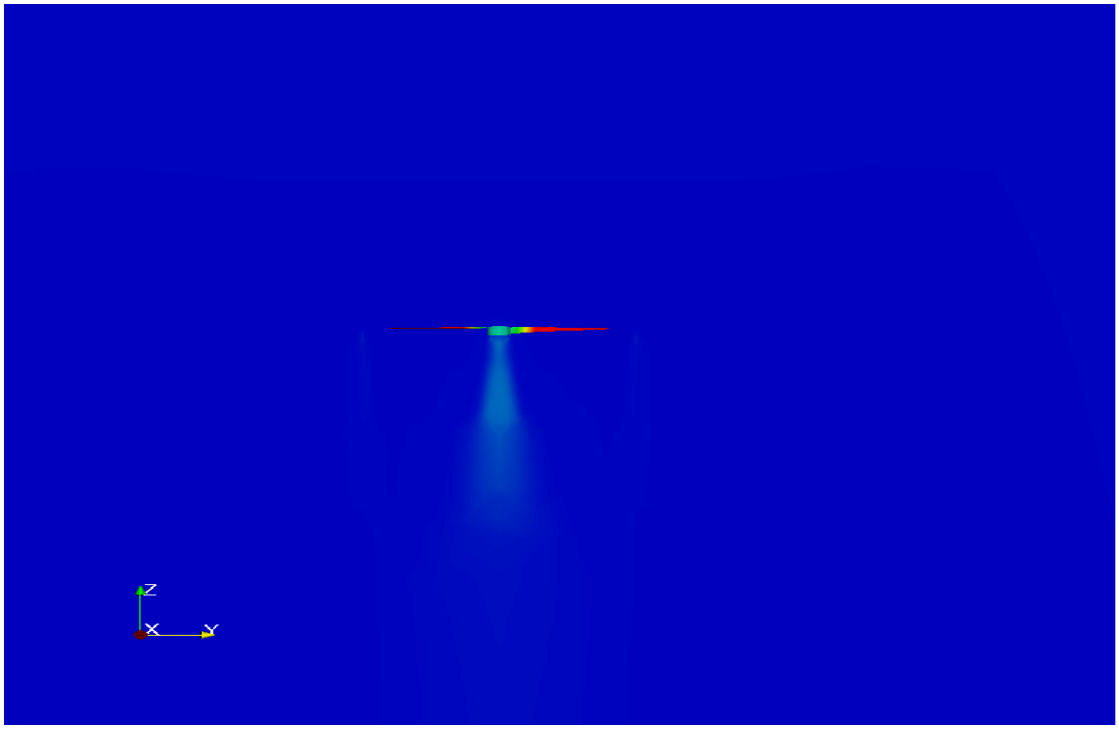

Figure 5.23: Propeller analysis at maximum speed with the help of OpenFoam. The figure above shows the vortices around the propeller. The flow is irrotational.

The results from both software match. The aircraft speed/engine speed diagram is depicted below.

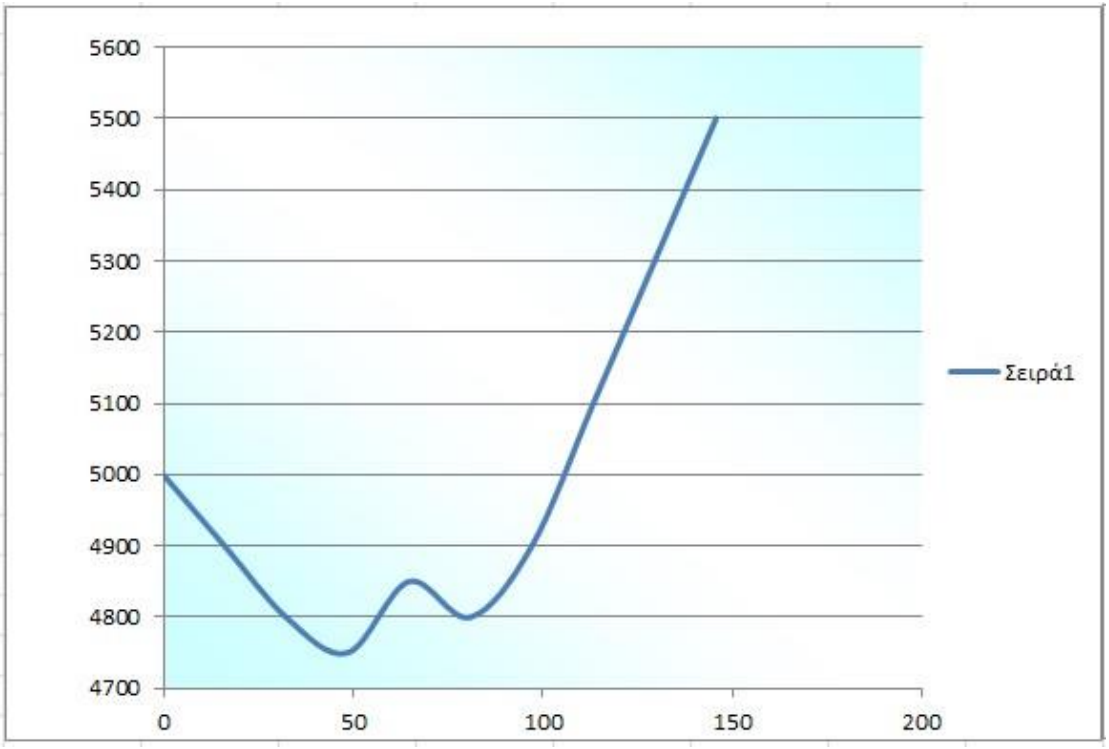

Figure 5.24: The diagram above shows the engine speed in relation to the aircraft's speed in km/hour as it resulted from the previous analysis. We easily notice the constant speed effect that was achieved thanks to the meticulous selection of the airfoil and the three-dimensional set.

6) Static and dynamic aero elasticity

A) Static aero elasticity

In an aircraft, two significant static aeroelastic effects may occur. Divergence is a phenomenon in which the elastic twist of the wing suddenly becomes theoretically infinite, typically causing the wing to fail spectacularly. Control reversal is a phenomenon occurring only in wings with ailerons or other control surfaces, in which these control surfaces reverse their usual functionality (e.g., the rolling direction associated with a given aileron moment is reversed).

i) Divergence occurs when a lifting surface deflects under aerodynamic load so as to increase the applied load, or move the load so that the twisting effect on the structure is increased. The increased load deflects the structure further, which eventually brings the structure to the diverge point. Divergence can be understood as a simple property of the differential equation(s) governing the wing deflection.

ii) Control reversal

Control surface reversal is the loss (or reversal) of the expected response of a control surface, due to deformation of the main lifting surface. For simple models (e.g. single aileron on an Euler-Benouilli beam), control reversal speeds can be derived analytically as for torsional divergence. Control reversal can be used to aerodynamic advantage, and forms part of the Kaman servo-flap rotor design.

With the help of the finite element program LISA and the OpenFoam, these two effects were tested and it was found that the aircraft is safe across the entire design speed rate. The wing stiffness is high and it is secured by the two effects above.

B) Flutter analysis

An analysis that included the influence of the time variable was performed in OpenFoam. In that way the non-steady load due to the aircraft's turbulence was calculated. The results for the wing (which are of high importance in the present analysis) are demonstrated below. Then, a modal analysis was made using the LISA program. The results stemming from the OpenFoam analysis were compared to the natural frequencies. There is no flutter at high speeds. A slight resonance was observed at high speeds, but according to the results from LISA the wing is able to withstand it. However, the maximum speed allowed was set well below this speed.

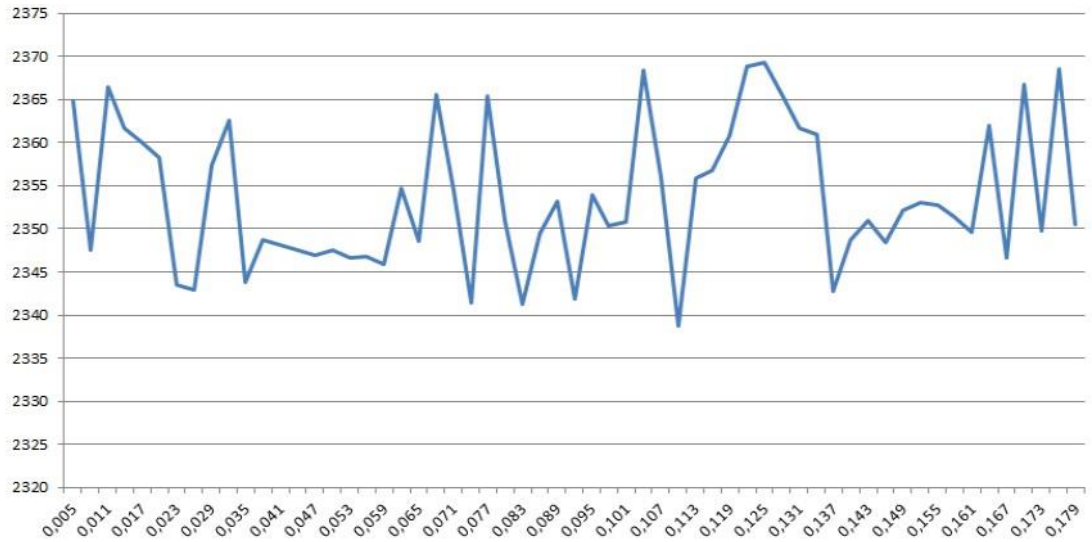

Figure 6.1: The figure above shows the results in reference to time when the aircraft flies at flutter speed.

The data above were analyzed using the LISA finite element program and after a circular process the analysis was completed. The figures below are from the analysis performed in LISA and they also include the aircraft's flight-envelope diagram.

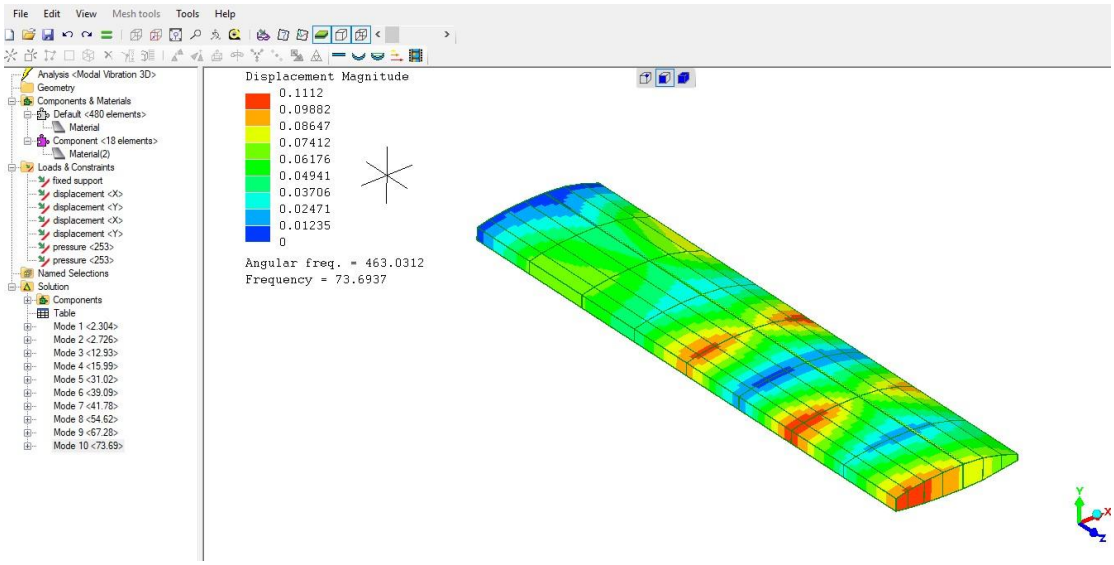

Figure 6.2: The figure above shows the maximum displacement for the 1st eigenvalue

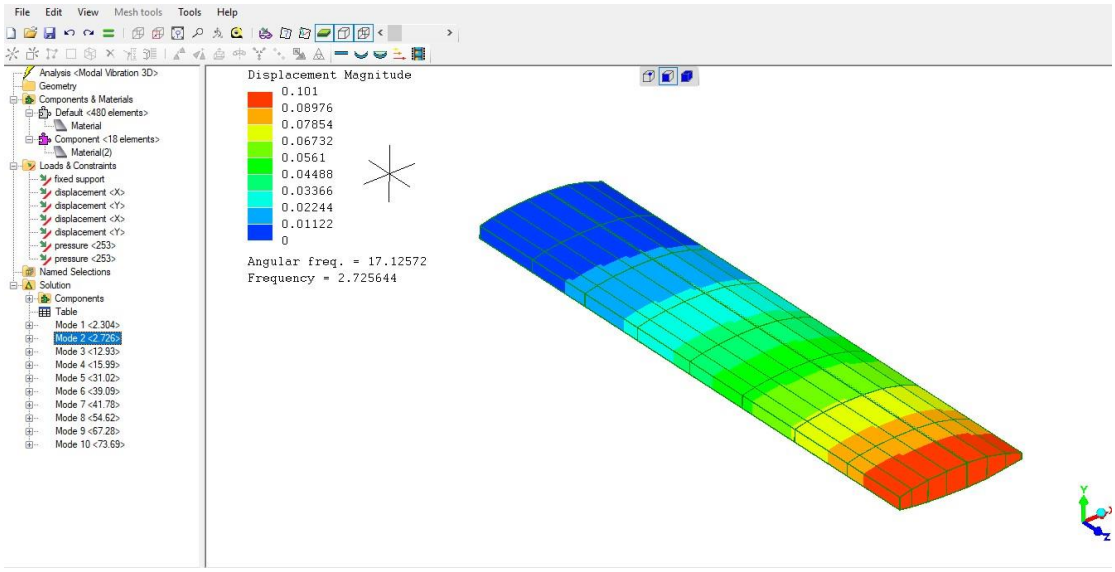

Figure 6.3: The figure above shows the maximum displacement for the 2nd eigenvalue

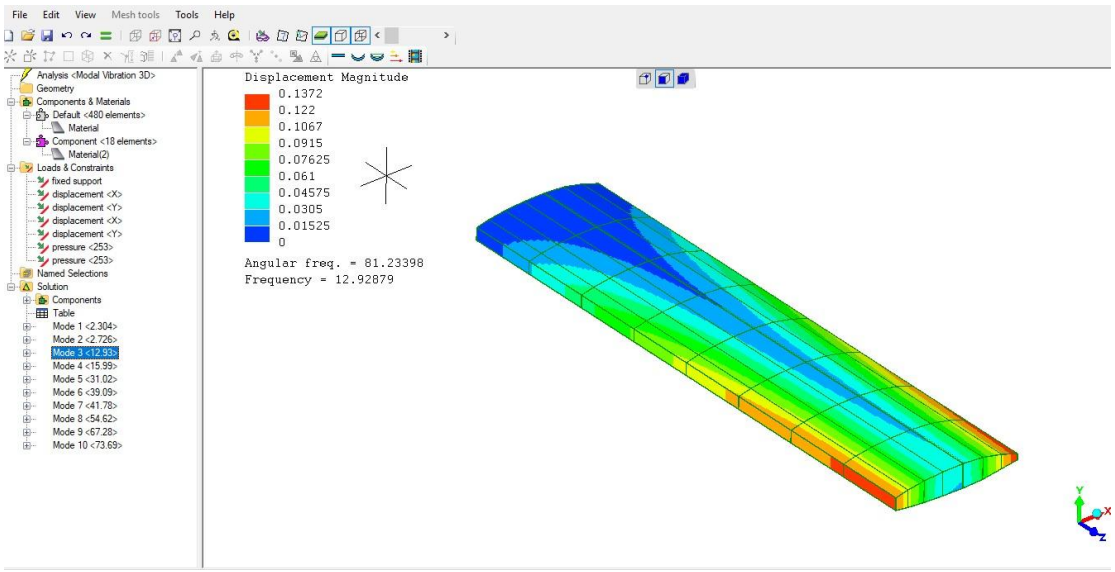

Figure 6.4: The figure above shows the maximum displacement for the 3rd eigenvalue

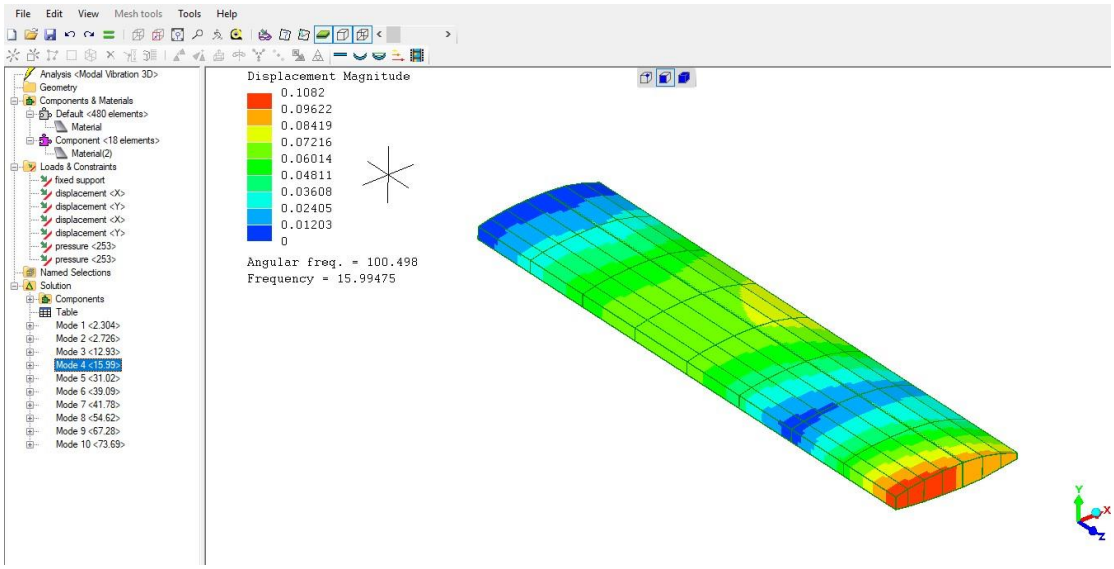

Figure 6.5: The figure above shows the maximum displacement for the 4th eigenvalue

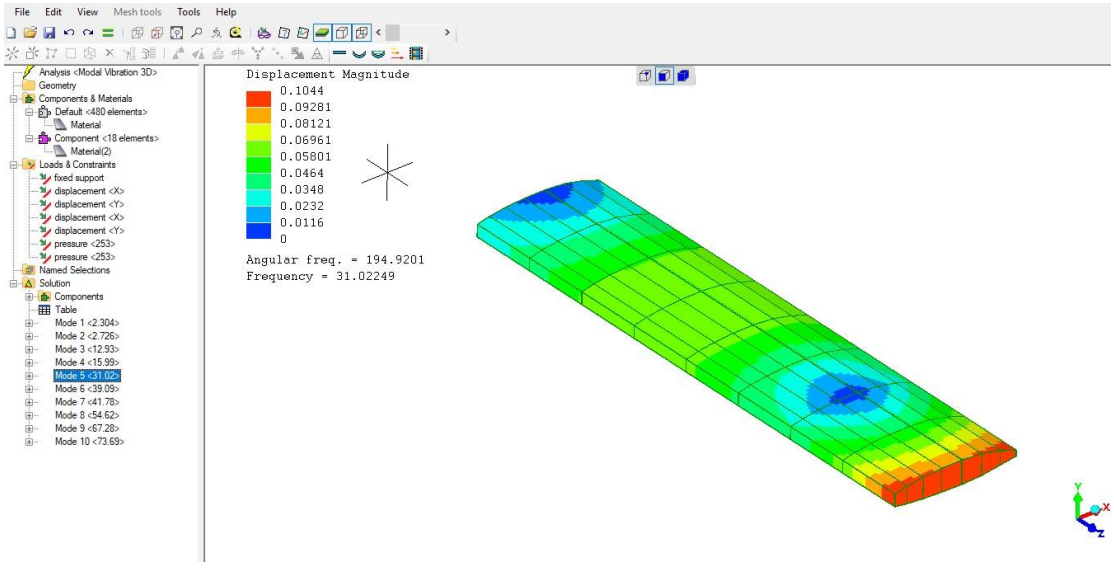

Figure 6.6: The figure above shows the maximum displacement for the 5th eigenvalue

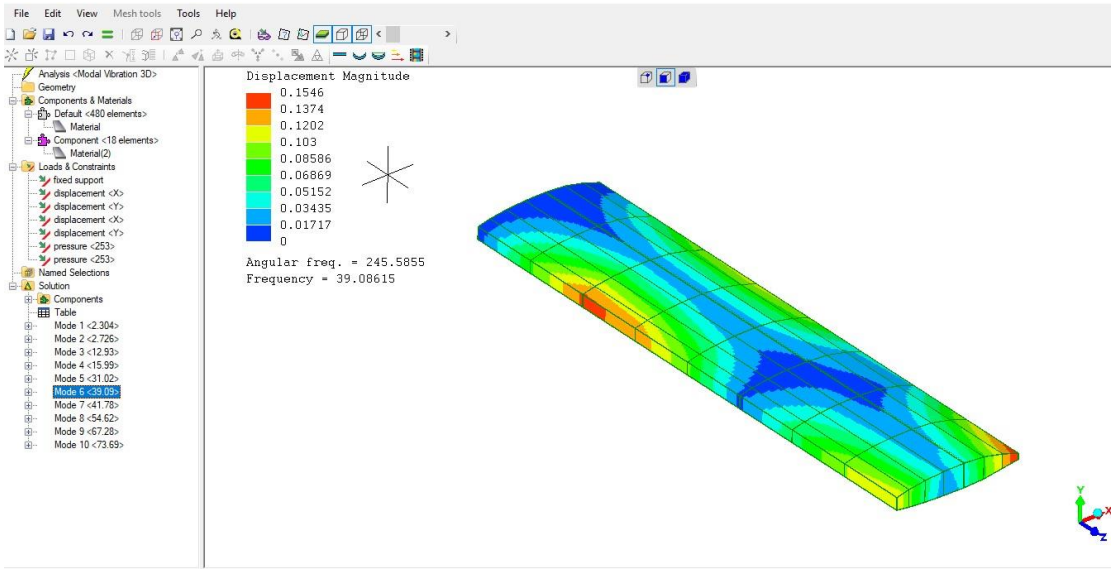

Figure 6.7: The figure above shows the maximum displacement for the 6th eigenvalue

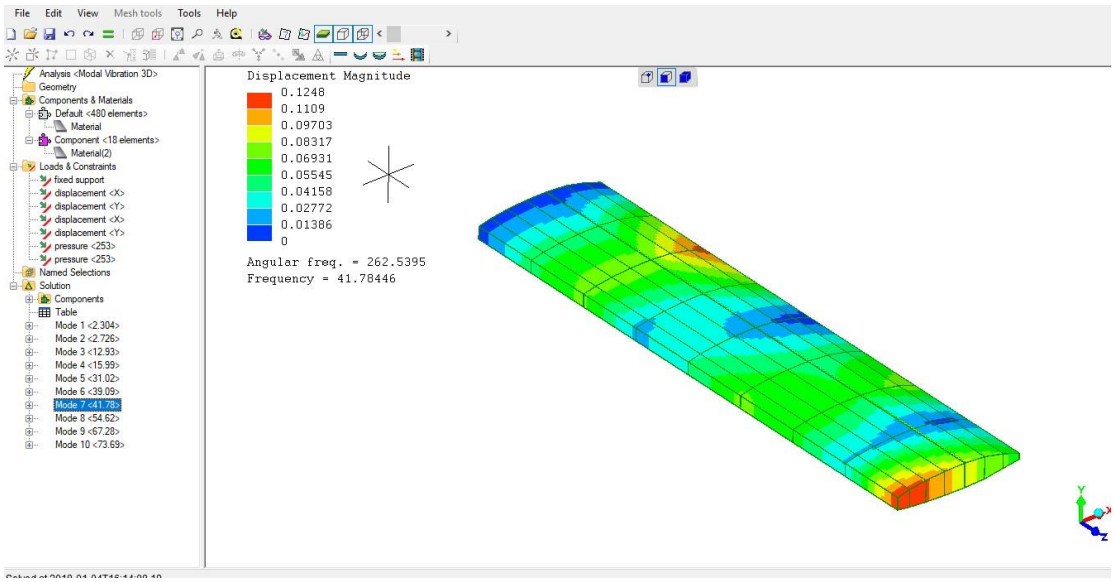

Figure 6.8: The figure above shows the maximum displacement for the 7th eigenvalue

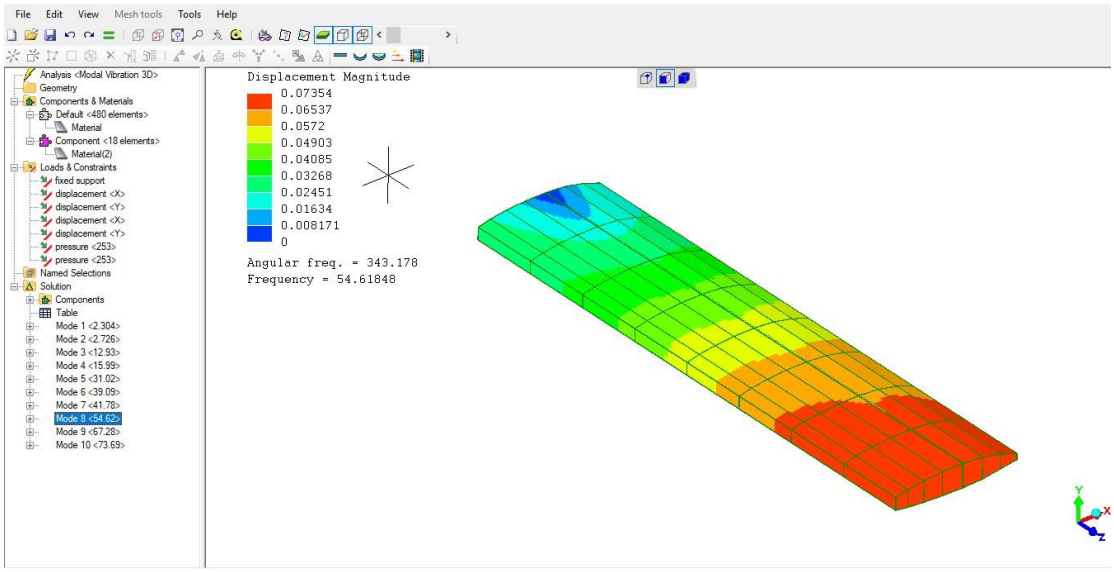

Figure 6.9: The figure above shows the maximum displacement for the 8th eigenvalue

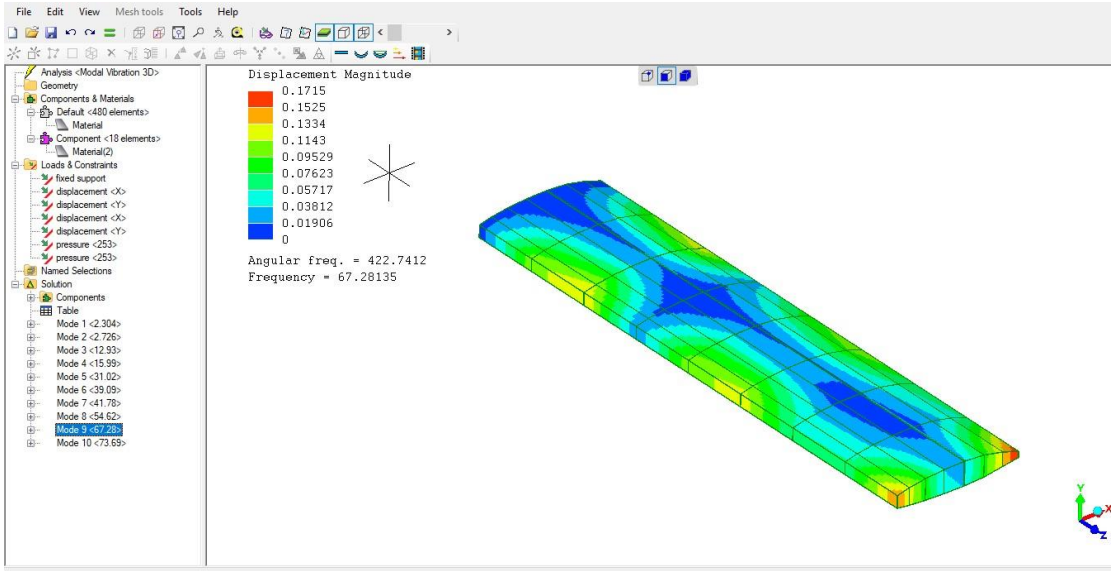

Figure 6.10: The figure above shows the maximum displacement for the 9th eigenvalue

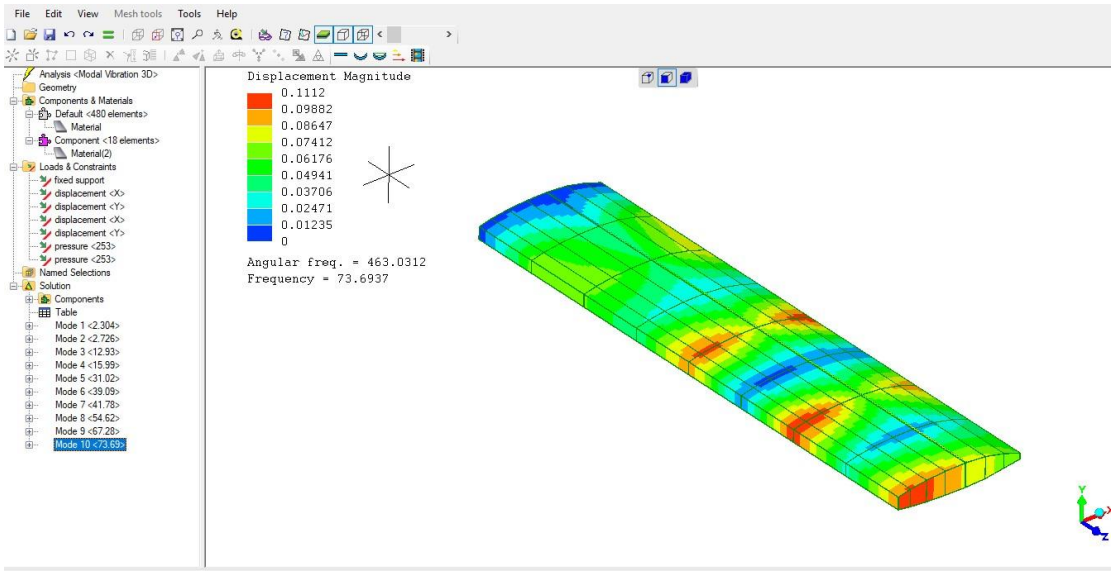

Figure 6.11: The figure above shows the maximum displacement for the 10th eigenvalue

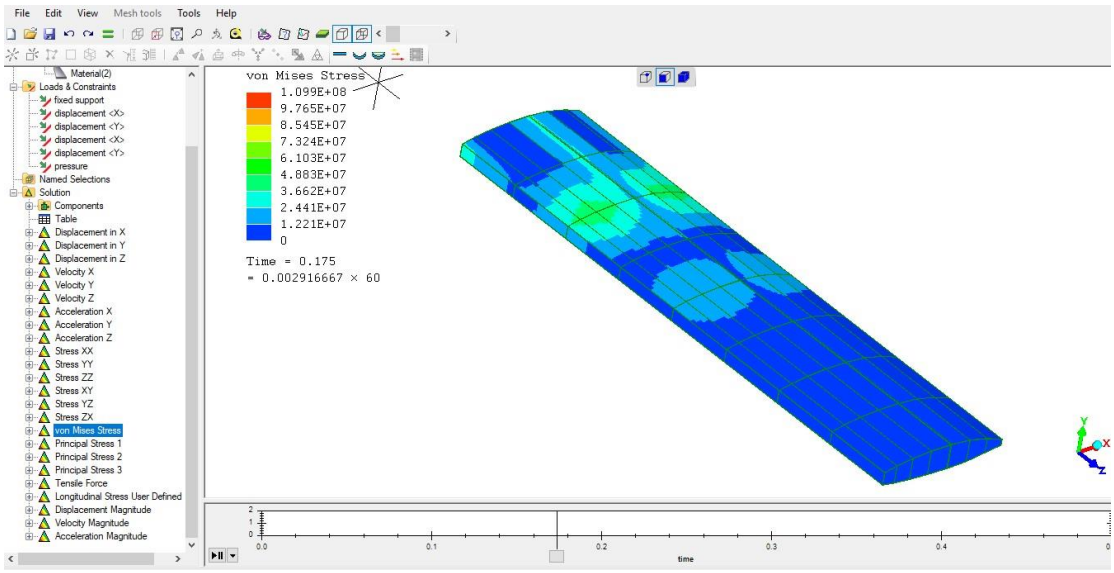

Figure 6.12: The figure above shows the stress forces resulting from a dynamic response analysis (for loads in flutter condition) in the LISA finite element program.

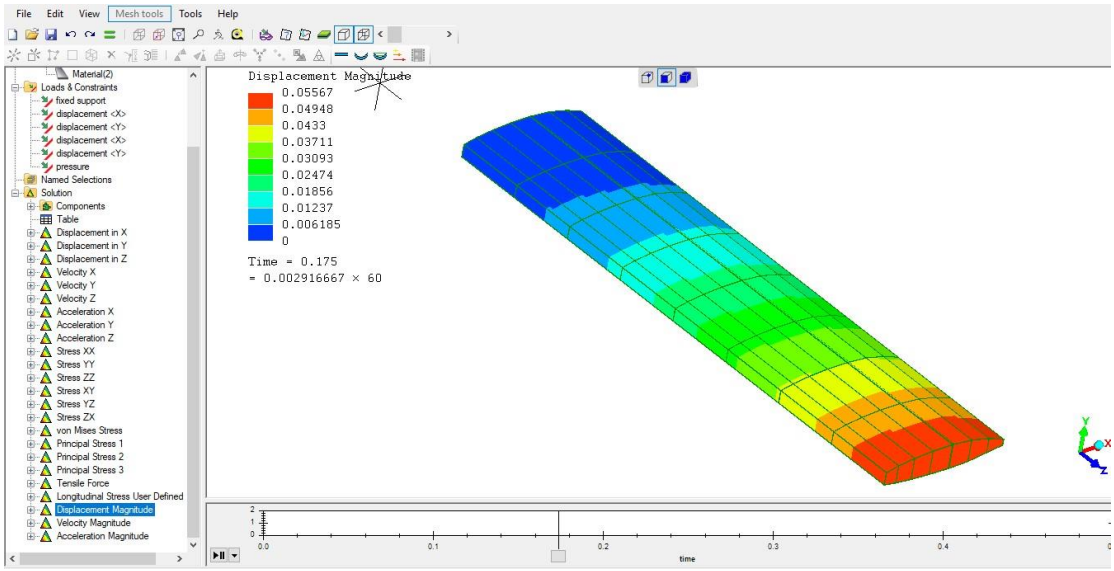

Figure 6.13: The figure above shows the displacement resulting from a dynamic response analysis (for loads in flutter condition) in the LISA finite element program.

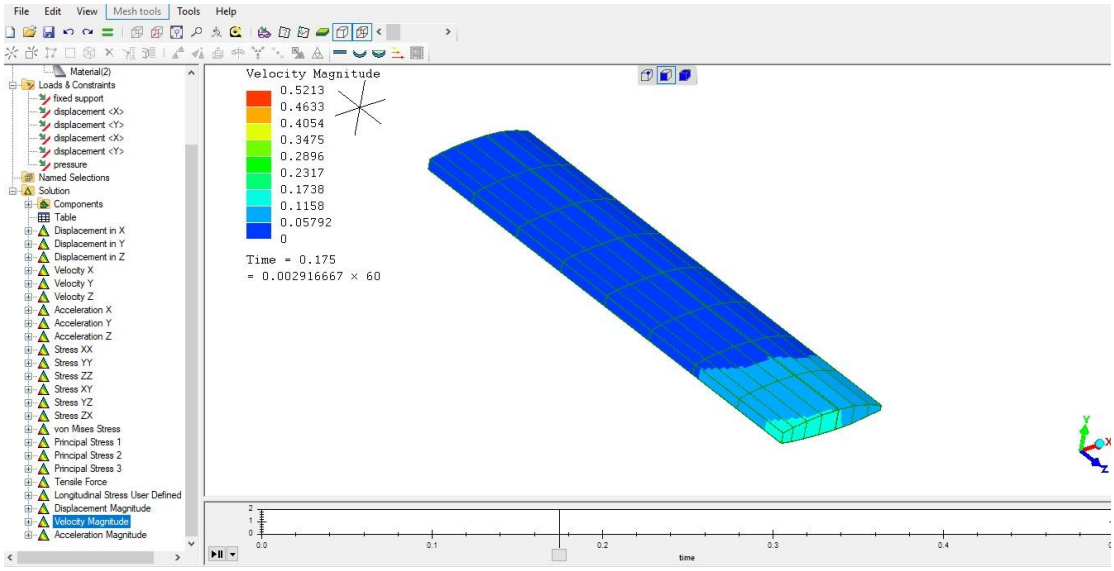

Figure 6.14: The figure above shows the speed resulting from a dynamic response analysis (for loads in flutter condition) in the LISA finite element program.

7) Airplane hard landing (as a result of stalling during flotation)

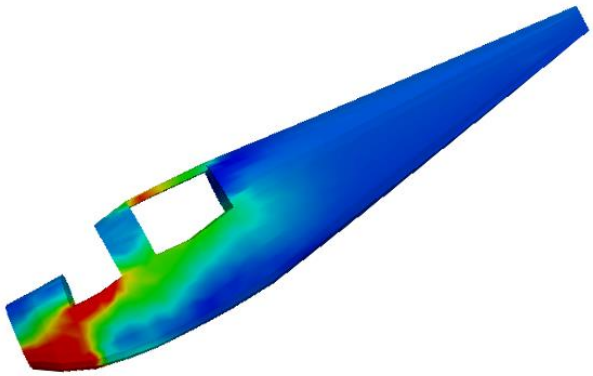

Figure 7.01: The figure above shows the stress forces resulting from a non-linear impact analysis in the Code_Aster finite element program. The stalling condition near the ground was emulated (using results from OpenFoam) and the worst case scenario was chosen (the height is such that the aircraft will be landed on the runway at a high angle speed but it is not sufficient enough for corrective flotation). The fuselage is strong enough to endure this while protecting the life of the passengers, however, in its front part there were areas that the material almost reached its strength resulting in extensive delamination damages, though which was acceptable as it helped absorb the collision energy.

8) Technical characteristics of aircraft

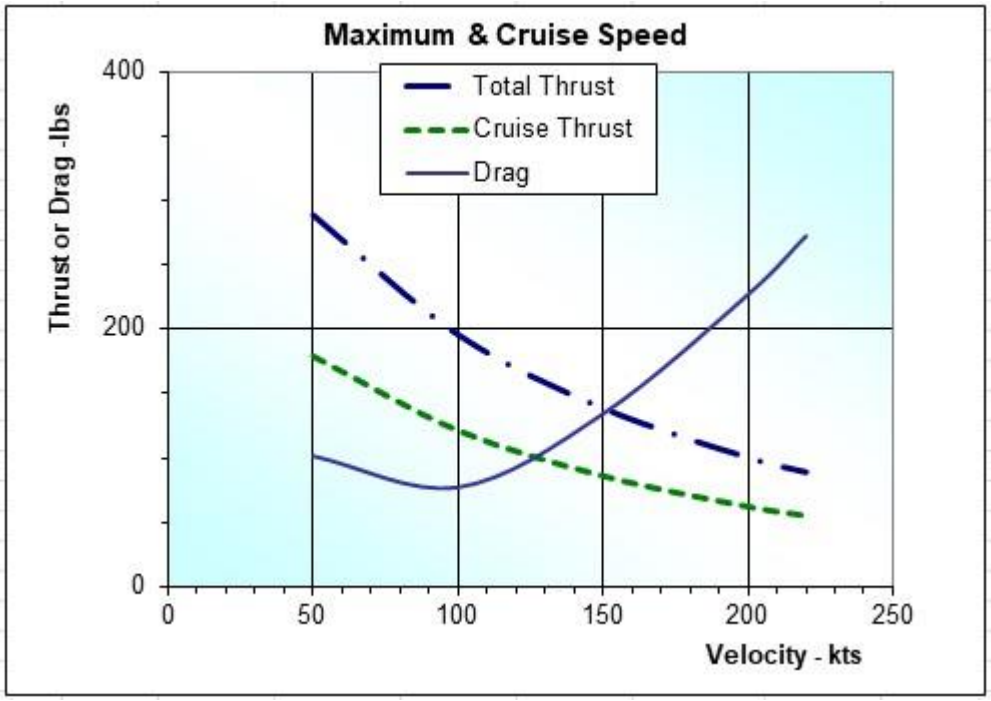

Figure 8.1: The figure above shows the thrust or drag in reference to velocity.

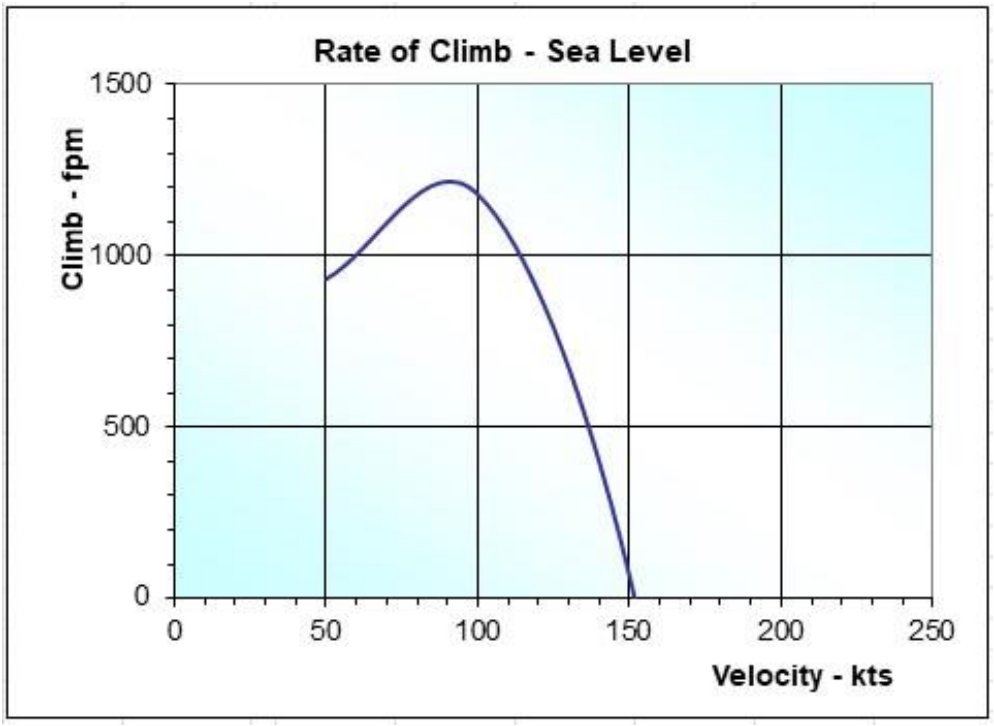

Figure 8.2: The figure above shows the rate of climb in reference to velocity.

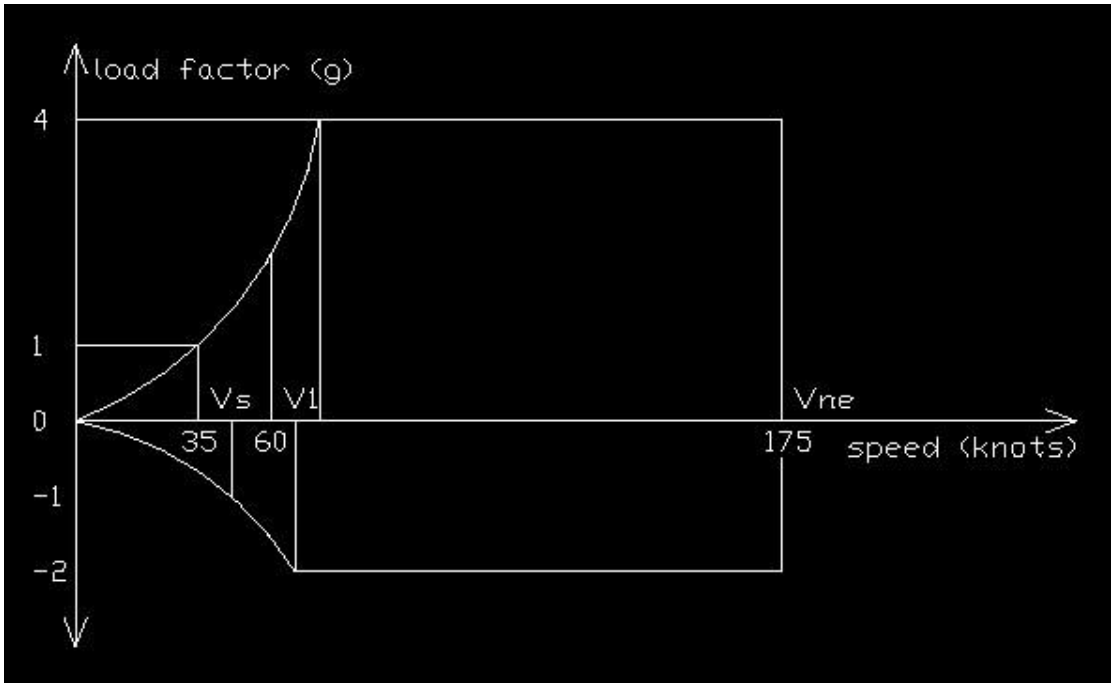

Figure 8.3: The figure above shows the flight envelope diagram of the aircraft.

The detailed technical characteristics of the aircraft are shown below, as they resulted from the analysis above.

Model	
Classification	Ultra-Light Airplane
General Layout	Conventional
Accommodations	2 seats
Airworthiness Requirements	
Aircraft Type	Multipurpose
Airframe	Composite
Wing Configuration	Low
Tail Configuration	Y-Fuselage mounted
Power Plant Configuration	Single-engine, Piston, Tractor, Fuselage mounted
Landing Gear Configuration	Fixed, Nose, Fuselage mounted
Length Overall	6,37 m
Height Overall	1,850 m
Total Wetted Area	44,888 m^2

WING

Area	9,900 m²
Span	9,000 m
Root chord	1,300 m
Tip chord	0,900 m
Tapered ratio	1,444
Aspect ratio	8,182
Longitudinal position on the fuselage	1,690 m
Sweep angle	0,0°
Sweep angle at 25% of wing chord	0,0°
Sweep angle at 50% of wing chord	0,0°
Dihedral	3,0°
Standard mean chord	1,100 m
Mean aerodynamic chord	1,120 m
Wetted area	17,617 m²
Ratio - Wing area vs Total wetted area	0,221
Ratio - Wing wetted area vs Fuselage wetted area	1,113
Ratio - Wing wetted area vs Total wetted area	0,392

FLAPERONS

Area	1,525 m²
Span (each)	3,850 m
Relative span (both)	85,50 %
Standard mean chord	0,202 m
Relative chord	18,00 %
Position along the wing span	0,650 m
Location along the span	14,44 %
Hinge axis relative position	9,0 %
Maximum down deflection	40,0°
Maximum up deflection	-15,0°
Ratio - Flaperon span vs Wing span	0,855

Ratio - Flaperon area vs Wing area	0,154

TAILS

Tails area	4,410 m²
Tails wetted area	8,952 m²
Tails area / Wing area	0,446
Ratio - Tails wetted area vs Total wetted area	0,203

HORIZONTAL TAIL

Type	Stabilizer and elevator
Area	2,810 m²
Span	2,950 m
Root chord	0,950 m
Tip chord	0,950 m
Tapered ratio	1,00
Aspect ratio	3,56
Longitudinal position on the fuselage	4,97 m
Sweep angle at leading edge	0,0°
Incidence	0,0°
Relative incidence	0,0°
Standard mean chord	0,950 m
Mean aerodynamic chord - Chord	0,950 m

AIRFOIL CHARACTERISTICS

Airfoil	NACA 66-009
Maximum relative thickness	9,1 %
Location of maximum relative thickness	45,0 %
Leading edge radius	0,7 %
Lift slope - airfoil	0,104/°
Airfoil - zero lift angle	-0,1°

Lift slope - Tail alone	0,074/°
Aerodynamic center position	5,328 m
Tail wetted area	1,666 m²
Ratio - Tail area vs Wing area	0,085
Ratio - Tail area vs vertical tail area	0,474
Ratio - Tail area vs Total wetted area	0,020
Ratio - Tail wetted area vs Wing wetted area	0,094
Ratio - Tail wetted area vs Fuselage wetted area	0,105
Ratio - Tail wetted area vs Total wetted area	0,038

ELEVATOR

Area	0,793 m²
Span	2,480 m
Relative span	84,0 %
Relative chord	35,0 %
Position along the span	0,177 m
Hinge axis position	10,0 %
Maximum down deflection	20,0°
Maximum up deflection	-30,0°
Ratio - Elevator span vs Horizontal tail span	0,840
Ratio - Elevator area vs Horizontal tail area	0,294

VERTICAL TAIL

Type	Fin and rudder
Area	1,600 m²
Span	1,600 m
Root chord	0,700 m
Tip chord	1,300 m
Tapered ratio	1,86
Aspect ratio	3,20
Longitudinal position on the fuselage	4,870 m

Root to tip sweep	23,20°
Standard mean chord	1,000 m
Mean aerodynamic chord - Chord	1,030 m
Tail moment arm	3,239 m

AIRFOIL CHARACTERISTICS

Airfoil	NACA 66-009
Maximum relative thickness	9,1 %
Location of maximum relative thickness	45,0 %
Leading edge radius	0,7 %
Lift slope - airfoil	0,104/°
Airfoil - zero lift angle	-0,1°

Lift slope - tail alone	0,046/°
Tail wetted area	3,248 m²
Ratio - Tail area vs Wing area	0,161
Ratio - Tail area vs Horizontal tail area	0,626
Ratio - Tail area vs Total wetted area	0,035
Ratio - Tail wetted area vs Wing wetted area	0,184
Ratio - Tail wetted area vs Fuselage wetted area	0,204
Ratio - Tail wetted area vs Total wetted area	0,074

RUDDER

Span	1,520 m
Relative span	95,0 %
Relative chord	40,0 %
Position along the span	0,070 m
Hinge axis position	50,0 %
Maximum left deflection	35,0°
Maximum right deflection	-35,0°
Ratio - Rudder span vs Vertical tail span	0,950

FUSELAGE	
Length	5,870 m
Maximum height	1,110 m
Maximum Width	1,120 m
Length of constant section	0,000 m
Fuselage frontal form coefficient	0,960
Fuselage lateral form coefficient	1,773
Fuselage frontal area	1,001 m²
Wetted area	15,833 m²
BASE	
Base frontal form coefficient	0,960
LANDING GEAR	
Base	1,519 m
Maximum tail down angle	8,0°
Wetted area	3,243 m²
MAIN GEAR	
Fixed gear	
Main gear - Tire	6.00-6
Main gear - Tire diameter	445 mm
Main gear - Tire width	160 mm
AUXILIARY GEAR	
Retractable gear	
Auxiliary gear - Tire	5.00-5
Auxiliary gear - Tire diameter	361 mm
Auxiliary gear - Tire width	126 mm
ENGINE	
Engine number	1

Engine model	Subaru EA-71
Engine - Specific fuel consumption	0,310 kg/kW.h
Engine - Specific weight	1,10 kg/kW
Maximum engine power	62,517 kW 85,0 hp
Maximum engine rpm	5750 t/min
Power-to-wing area ratio	5,62 kW/m²
Power-to-weight ratio	0,139 kW/kg
Weight-to-power ratio (Power loading)	7,198 kg/kW

PROPELLER

Number of propeller	1
Type	Fixed pitch
Material	Wood
Number of blades	2
Propeller pitch angle - Minimum	16,0°
Propeller pitch angle - Maximum	46,0°
Propeller diameter	1,700 m
Disc area	2,269 m²
Maximum disc loading	27,55 kW/m²
Maximum disc loading vs Number of blades	13,76 kW/m²
Spinner - Diameter	0,200 m
Spinner - Length	0,210 m

MOMENT OF INERTIA (ESTIMATED)

Fuel system - Main tank location	Wing
Fuel system - Location	Wing
Fuel system - Capacity	20.l
Fuel system - Location	Wing
Fuel system - Capacity	20.l
Fuel system - Maximum fuel capacity	40.l
Wing tank capacity	40.l

WEIGHT AND LOADING

Maximum Takeoff weight	450,0 kg
Empty weight	253,9 kg
Flight weight	450,0 kg
Useful weight	196,1 kg
Weight of crew - Unit	86,0 kg
Weight of crew - Total	172,0 kg
Weight of freight - Unit	5,0 kg
Weight of freight - Total	10,0 kg
Weight of fuel	33,5 kg
Weight of crew - Minimum	50,0 kg
Weight of fuel - Minimum	10,0 kg
Minimum Takeoff weight	313,9 kg
Power plant	65,0 kg
Engines(1)	65,0 kg
Propellers(1)	4,0 kg

COMPUTED WEIGHT

Wing	65 kg
Horizontal tail	12,2 kg
Vertical tail	12,5 kg
Fuselage	45 kg
Main landing gear	8 kg
Auxiliary landing gear	5 kg
Engines(1)	65,0 kg
Propellers(1)	4 kg
Fuel system	5,3 kg
Control system	8,9 kg
Electrical system	10,0 kg
Instruments	3,0 kg

Furnishings	10,0 kg
Empty weight	253,9 kg

CENTRE OF GRAVITY POSITION

Occupant(1)	2,020 m
Occupant(2)	2,020 m
Freight	2,570 m
Fuel	1,960 m
Batteries (M)	1,030 m
Wing	2,250 m
Horizontal tail	5,300 m
Vertical tail	5,660 m
Fuselage	2,340 m
Main landing gear	2,540 m
Auxiliary landing gear	1,910 m
(1)Engine	0,770 m
(1)Propeller	0,250 m
Fuel system	1,820 m
Control system	2,080 m
Electrical system	1,450 m
Instruments	1,280 m
Furnishings	1,930 m
Flight weight	450,0 kg

MASS CORRECTION FACTOR

General	1,000

MISSION SEGMENT WEIGHT FRACTION

[1] Warm-up	1,000
[2] Taxi	1,000
[3] Takeoff	1,000

[4] Climb	0,997
[5] Cruise	0,906
[6] Descent	1,000
[7] Loiter	1,000
[8] Descent	1,000
[9] Landing	1,000
[10] Taxi	1,000

WEIGHT RATIO

Ratio - Empty weight vs Maximum Takeoff weight	0,564
Ratio - Useful weight vs Maximum Takeoff weight	0,436
Ratio - Fuel weight vs Maximum Takeoff weight	0,074
Ratio - Useful weight vs Empty weight	0,772
Ratio - Fuel weight vs Empty weight	0,132
Ratio - Fuel weight vs Useful weight	0,171
Ratio - Weight of engine vs Empty weight	0,256
Ratio - Empty weight vs Wing area	25,647 kg/m²
Ratio - Maximum Takeoff weight vs Wing area	45,455 kg/m²
Ratio - Empty Weight vs Total wetted area	6,530 kg/m²
Ratio - Maximum Takeoff Weight vs Total wetted area	11,574 kg/m²

AERODYNAMICS

Maximum lift coefficient (Dirty)	2.35
Maximum lift coefficient (Clean)	1,55
Maximum lift increment	0,80
Wing loading at maximum Takeoff weight	45,455 kg/m²
Wing loading at empty weight	25,647 kg/m²
Friction coefficient, Coefficient (power flight)	0,00530
Friction coefficient, Reference altitude	0.m

QUALITY CRITERIA	
Fuel consumption (cruise)	6,27 l/100km
FLIGHT AT MAX CONTINUOUS SPEED	
Flight speed	245 km/h
- Ground speed (GS)	245 km/h
- True Air Speed (TAS)	245 km/h
- Indicated Air Speed (IAS)	218 km/h
Airplane CG rel. position (%CMA)	28,00 %
Wing loading	45,455 kg/m²
Flight weight	450,0 kg
Flight altitude	2400.m
Range	384 km
Endurance	1 h 33 min
Time to climb	7 min 52 s
Power, maximum	62,157 kW
Power, available	62,000 kW
Power, required	60,000 kW
Engine relative power	96,5 %
Specific fuel consumption	0,310 kg/kW.h
Engine rpm	5500 t/min
Propeller - rpm	2750 t/min
Propeller - Pitch angle	24,25°
Propeller - Efficiency	85,0 %
Propeller - Thrust (net)	1489 N
RATE OF CLIMB	
MAXIMUM RATE OF CLIMB	
Flight weight	450,0 kg
Flight altitude	0.m

Rate of climb	6,1 m/s
Flight speed	165 km/h
- Ground speed (GS)	165 km/h
- True Air Speed (TAS)	165 km/h
- Indicated Air Speed (IAS)	165 km/h
Power, maximum	62,157 kW
Power, available	62,000 kW
Propeller - rpm	2400 t/min
Propeller - Pitch angle	24,25°
Propeller - Efficiency	79,47 %
Propeller - Thrust (net)	1095 N
Propeller - Thrust-to-Power ratio	17,66 N/kW
Climb angle	7,58°
Climb slope	13,43 %

TAKEOFF

Airplane CG rel. position (%CMA)	28,0 %
Runway surface	Concrete
Takeoff run	185.m
Takeoff distance to 15m	284.m
Takeoff weight	450,0 kg
Flight altitude	0.m
Wing trailing edge deflection angle	10,0°
Runway slope	0,0 %
Front wind speed	0 km/h

At rotation speed

Stall speed	71,5 km/h
Takeoff speed	120 km/h
Lift coefficient (maximum)	1,88
Lift coefficient	0,68

Mean acceleration	2,96 m/s²
Runway surface	grass
Takeoff run	236.m
Takeoff distance to 15m	335.m
Takeoff weight	450,0 kg
Flight altitude	0.m
Wing trailing edge deflection angle	10,0°
Runway slope	0,0 %
Front wind speed	0 km/h

LANDING

Airplane CG rel. position (%CMA)	28 %
Runway surface	Concrete
Landing weight	450,0 kg
Flight altitude	0.m
Wing trailing edge deflection angle	40,0°
Runway slope	0,0 %
Front wind speed	0 km/h
Breakdown	
Speed, approach	125 km/h
Speed, flare out	102 km/h
Speed, touch down	95 km/h
Landing, brakes OFF	
Distance from the obstacle (15m)	565.m
Distance during approach	90.m
Distance during flare out	35.m
Distance during touch down	40.m
Distance during ground roll	400.m
Mean deceleration	0,844 m/s²
Landing, brakes ON	
Distance from the obstacle (15m)	260.m

Distance during approach	90.m
Distance during flare out	35.m
Distance during touch down	40.m
Distance during ground roll	95.m
Mean deceleration	3,76 m/s²

BEST RANGE

Range	915 km
Flight altitude	2400.m
Flight speed	182 km/h
- Ground speed (GS)	182 km/h
- True Air Speed (TAS)	182 km/h
- Indicated Air Speed (IAS)	162 km/h
Airplane CG rel. position (%CMA)	28 %
Flight speed (optimal) (104,4 kg/m²)	182 km/h
Endurance	5 h 2 min
Flight weight	450,0 kg
Wing loading	45,455 kg/m²
Wing loading (optimal) (182 km/h)	45,455 kg/m²
Power, maximum	62,157 kW
Power, available	62,000 kW
Power, required	22,000 kW
Engine relative power	35,5 %
Specific fuel consumption	0,300 kg/kW40,467.h
Propeller - rpm	1950 t/min
Propeller - Pitch angle	24,25°
Propeller - Efficiency	79,55 %

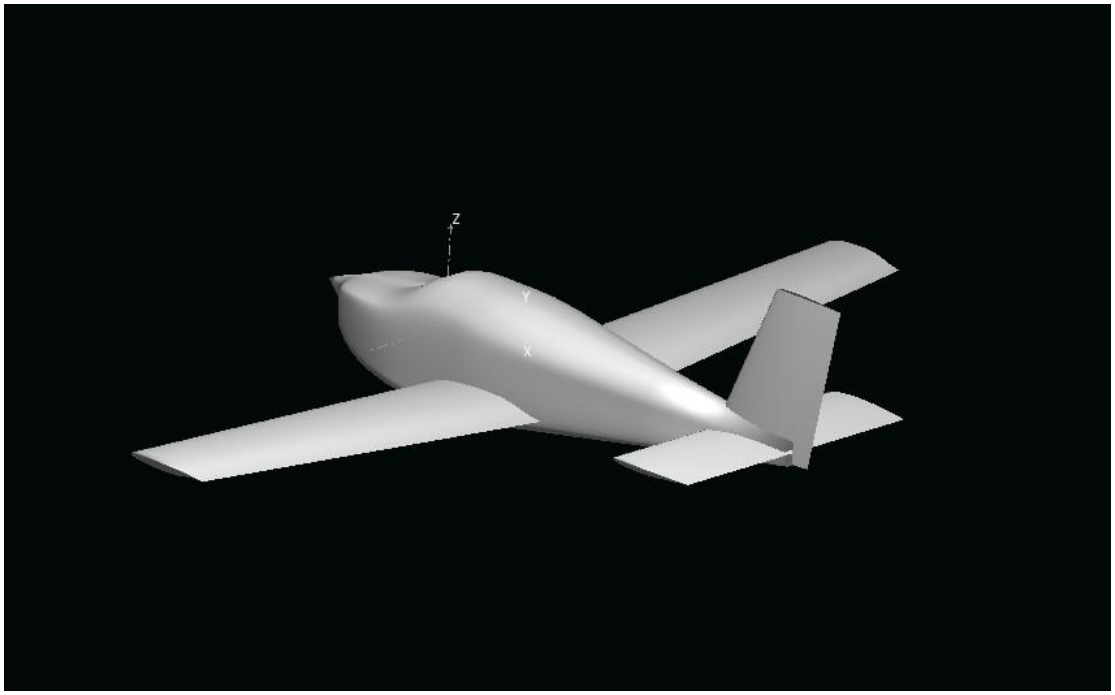

Figure 8.4: 3d view of the aircraft.

STABILITY

LONGITUDINAL DERIVATIVES

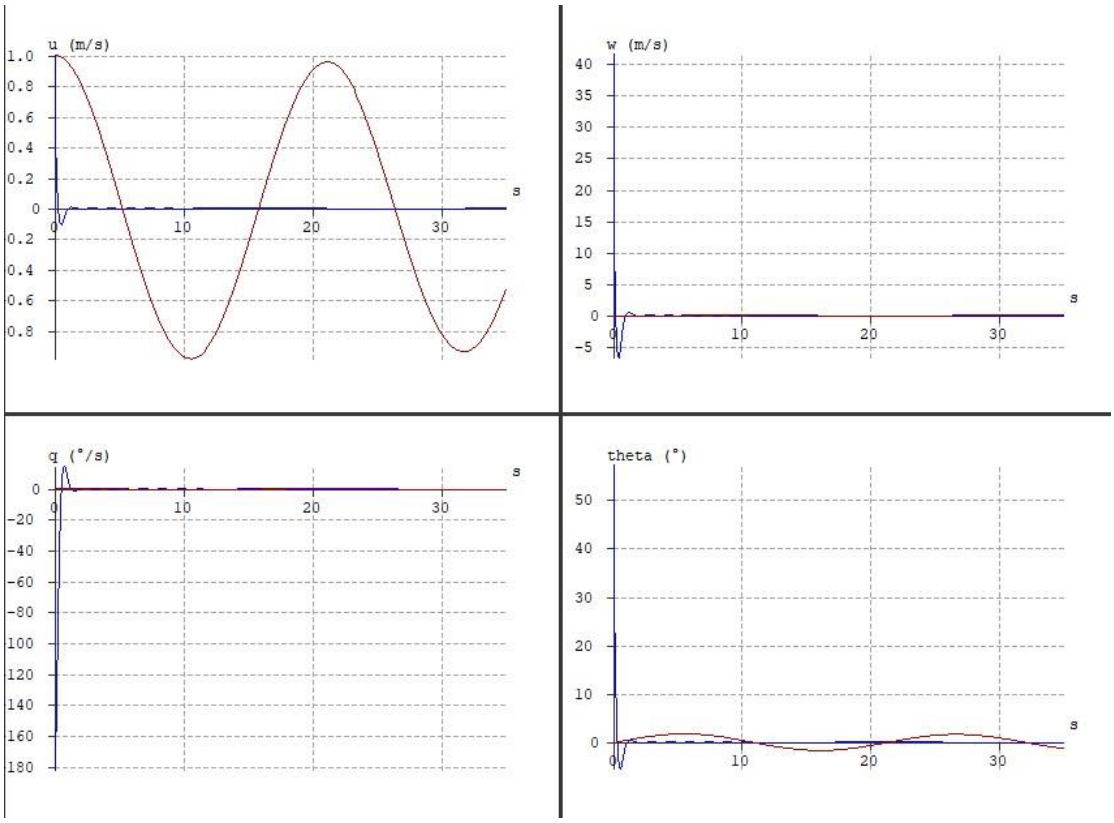

LATERAL DERIVATIVES

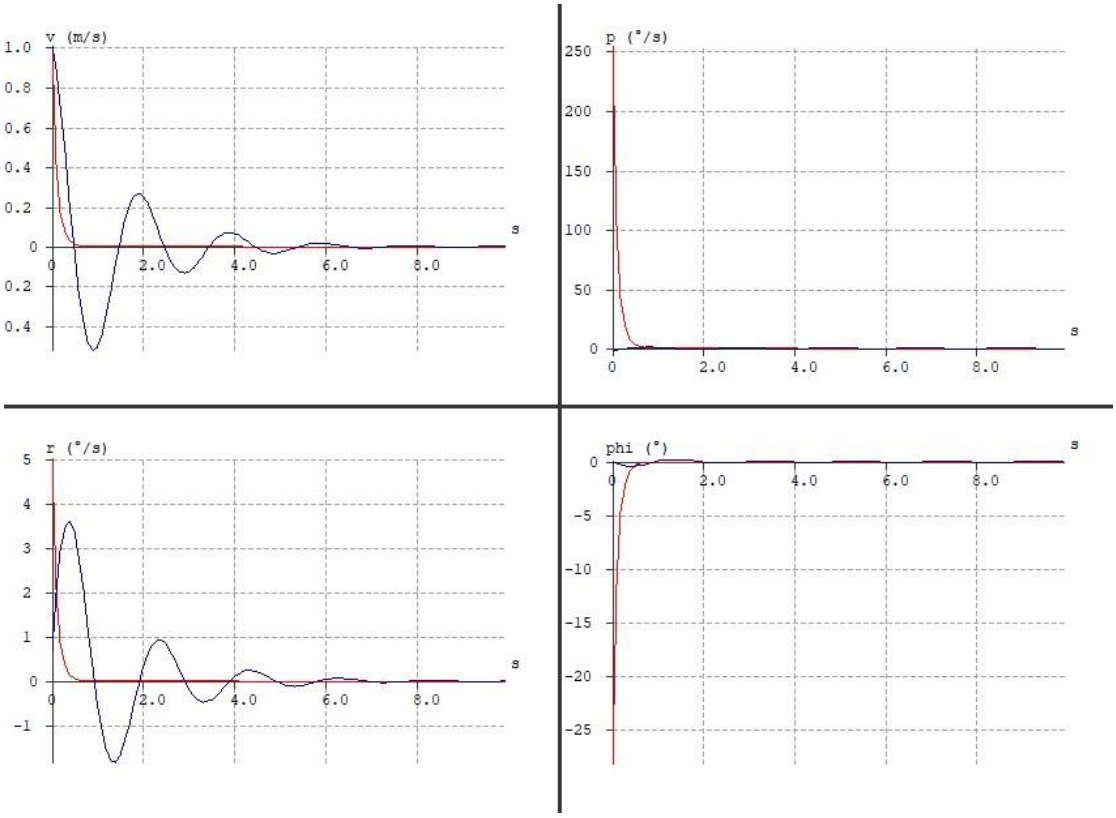

Acknowledgment

I'd like to thank LISA's technical support

I also want to thank the outstanding engineer and scientist Paul Martin for his expertise, advice and guidance throughout the study.

It was an honor to be given the opportunity to have those two gentlemen above significantly contribute to this study.

I would also like to thank my instructor (Giannis Bouloubasis) who not only made me an air operator, but also helped me understand how the aircraft functions and, through his very own, first-hand experience, assisted me in setting up this one.

Designer: Christos Anastasopoulos (Civil engineer with certification in computational fluid dynamics and undergraduate pilot).

Design and construction of civil engineering projects.

email: xrisanast@gmail.com